Table 1. Fatty Acid Contents for a Rat in Dosing Solvent (mg)

Groups		16:0 Palmitic acid	18:0 Stearic acid	18:1 Oleic acid	18:2 Linoleic acid	20:1 Gadoleic acid	20:4(n-6) AA	20:5 EPA	22:5 DPA	22:6 DHA	Other FA	tocopherol	Total
1,6	128 mg 97% purify DHA-E	0.0	0.0	0.0	0.0	0.0	0.0	0.0	0.0	120.0	4.0	4.0	128.0
2,7	404 mg 30% purify DHA-TG	56.8	13.6	74.0	5.2	10.0	8.0	32.8	12.0	113.2	74.4	4.0	404.0
3	128 mg 30% purify DHA-TG	17.6	4.2	22.9	1.6	3.1	2.5	10.2	3.7	35.1	23.1	4.0	128.0
4	4 mg tocopherol	0.0	0.0	0.0	0.0	0.0	0.0	0.0	0.0	0.0	0.0	4.0	4.0

AA: arachidonic acid. EPA: eicosapentaenoic acid. DPA: docosapentaenoic acid. FA: Fatty acid.

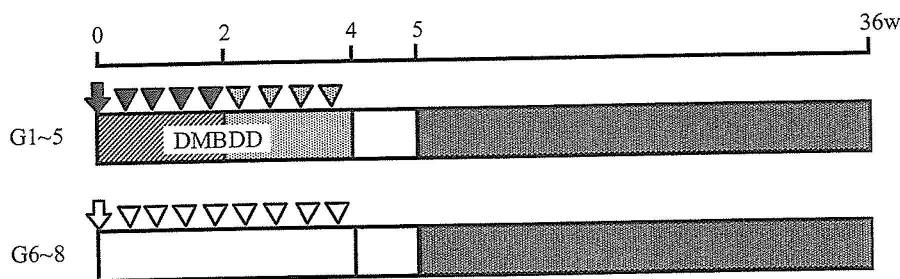

Fig. 1. Experimental protocol for the medium-term multi-organ carcinogenesis model. Animals: male F344/DuCrj rats, 6 weeks old; ⬇, DEN, 100 mg/kg body wt. i.p.; ▼, MNU, 20 mg/kg body wt. i.p.; ▽, DMH, 40 mg/kg body wt. s.c.; ▨, BBN, 0.05% in drinking water; □, DHPN, 0.1% in drinking water; ⇩▽, saline injection; ▩, G1 and 6, 128 mg 97% purity DHA-E, G2 and 7, 404 mg 30% purity DHA-TG, G3, 128 mg 30% purity DHA-TG, G4, 4 mg tocopherol, G5 and 8, no treatment.

therefore important to examine modification potential not in a single organ, but rather in the whole body. This requires *in vivo* experimental models which can detect effects in a wide spectrum of organs, and for this purpose several multi-organ wide-spectrum initiation models have been established[11–14]. The medium-term approach has clear benefits for the examination of modifying effects of chemicals in multiple organs in a single experiment within a relatively short experimental period[15–17] and is based on the proven good agreement between the multi-organ carcinogenesis model and long-term experimental results[18].

The ethyl ester formed by DHA (DHA-E) has been used in many chemoprevention studies[1–6], and DHA-TG has been used in a clinical trial study[7]. Therefore, we thought it important to investigate the difference in the modifying effects on carcinogenesis of DHA-E and DHA-TG. In the present study, we investigated the post-initiation-phase modifying activity of DHA-E and DHA-TG at the whole organ level using a rat medium-term multi-organ carcinogenesis model developed in our laboratory[8,15,19,20]. Furthermore, a tocopherol group was included as a comparative control.

Materials and Methods

Animals

Male F344 rats, aged 5 weeks, were obtained from Charles River Japan Inc. (Kanagawa Japan), and housed five to a plastic cage with wood chips for bedding in an air-conditioned room at 22 ± 2°C with a 12-h light: 12-h dark cycle. They were maintained on Oriental MF diet (Oriental Yeast Co., Tokyo, Japan) and tap water *ad libitum*. The study was started after 1 week of acclimatization.

Chemicals

N-Diethylnitrosamine (DEN), *N*-methyl-*N*-nitrosourea (MNU), 1,2-dimethylhydrazine (DMH) and *N*-butyl-*N*-(4-hydroxybutyl)nitrosamine (BBN) were obtained from Tokyo Kasei Kogyo Co., Ltd. (Tokyo, Japan) and dihydroxy-di-*N*-propylnitrosamine (DHPN) was obtained from Nacalai Tesque Co. (Osaka, Japan). The DHA dosing solution was supplied by Nippon Suisan Kaisha, Ltd. (Tokyo, Japan). DHA naturally exists in fish oil as a triglyceride (DHA-TG). DHA-E was chemically synthesized from DHA-TG by removing other fatty acids such as oleic acid and EPA. The contents in the dosing solution used in the present study are shown in Table 1. They were stored in sealed ampules under anaerobic conditions at –20°C in the dark.

Experimental methods

Medium-term multi-organ carcinogenesis study

The experimental protocol is shown in Fig. 1. The animals were randomly allocated to 8 groups of 10 – 20 animals. Those in groups 1 to 5 received the combined carcinogen treatments, consisting of a single *i.p.* injection of 100 mg/kg body wt. of DEN, four *i.p.* injections of 20 mg/kg body wt. of MNU, four *s.c.* injections of 40 mg/kg body wt.

Table 2. Final Body and Organ Weights Data

Groups	DMBDD	Treatment	Effective no. of rats	Body wt.[a)] (g)	Liver wt.[a)] (g)	Liver wt.[a)] (%, b.w.)	Kidneys wt.[a)] (g)	Kidneys wt.[a)] (%, b.w.)
1	+	128 mg 97% DHA-E	19	312.4 ± 14.8[b)]	6.60 ± 0.45	2.11 ± 0.08	2.00 ± 0.44	0.64 ± 0.15
2	+	404 mg 30% DHA-TG	17	318.6 ± 15.5	7.01 ± 0.51	2.23 ± 0.11[c)d)]	3.12 ± 3.15	1.00 ± 1.00
3	+	128 mg 30% DHA-TG	19	306.8 ± 20.5[c)]	6.53 ± 0.59	2.13 ± 0.09	2.03 ± 0.65	0.67 ± 0.25
4	+	4 mg Tocopherol	18	314.8 ± 24.7	6.74 ± 0.54	2.14 ± 0.10	1.97 ± 0.22	0.62 ± 0.06
5	+	no treatment	19	324.6 ± 18.2	6.83 ± 0.47	2.10 ± 0.08	2.03 ± 0.36	0.63 ± 0.11
6	–	128 mg 97% DHA-E	10	356.6 ± 18.2	7.56 ± 0.71	2.13 ± 0.24	1.93 ± 0.16	0.54 ± 0.02
7	–	404 mg 30% DHA-TG	10	373.0 ± 11.7	7.80 ± 0.24	2.09 ± 0.06	2.05 ± 0.11	0.55 ± 0.03
8	–	no treatment	10	369.5 ± 14.9	7.61 ± 0.36	2.06 ± 0.05	2.00 ± 0.11	0.54 ± 0.03

a) Mean ± SD.
b), c) Significantly different from group 5 at P<0.05 and 0.01, respectively.
d) Significantly different from group 4 at P<0.05.

of DMH, together with 0.05% BBN for 2 weeks and then 0.1% DHPN for 2 weeks (both given in the drinking water), during the initial 4 week period for multiple initiation (DMBDD treatment) as described previously[21–23]. Animals in groups 1 to 5 were then given intragastric injections, 1 ml of 128 mg/ml of 97% purity DHA-E, 404 mg/ml of 30% purity DHA-TG, 128 mg/ml of 30% purity DHA-TG, each with 4 mg/ml of tocopherol, or tocopherol alone or distilled water, 3 times a week from 1 week after completion of the DMBDD treatment to the end of the experiment. Animals in groups 6 to 8 were given 128 mg/ml 97% purity DHA-E, 404 mg/ml 30% purity DHA-TG and distilled water as a solvent control without DMBDD treatment from week 5. The treatment times per week and concentration of DHA dosing solution were decided according to a trial study[7]. Animals were weighed once a week in the initial 14 weeks, then once every 2 weeks until the end of the study period, at week 36, when all surviving animals were sacrificed by exsanguination under ether anesthesia and subjected to complete necropsy.

All experimental procedures were performed in accordance with the in-house guideline for the Care and Use of Laboratory Animals at DIMS Institute of Medical Science.

Aberrant crypt foci assay

Nine or 10 rats for each treatment with DMBDD initiation and 5 rats each without DMBDD were analyzed for colon ACF. The colon was removed, slit open from the anus to the cecum along the longitudinal axis, flattened between sheets of filter paper, and fixed in buffered 10% formalin. Then it was stained with 0.2% methylene blue solution by the procedure of Bird[24] to observed aberrant crypts. The number of aberrant crypt foci per colon, the number of aberrant crypts in each focus, and the location of each focus was determined by microscopy.

Histopathological examination

At necropsy, the brain, liver, kidneys, spleen, heart, lungs, thymus, testes and adrenals were excised and weighed, and the relative percentage organ weights were calculated on the basis of final body weights. These and the other major organs including small and large intestines were fixed in 10% buffered formalin, and routinely processed. Paraffin-embedded sections were stained with hematoxylin and eosin for histopathological examination. Liver slices fixed in 10% buffered formalin were also prepared for quantitative assessment of immunohistochemically demonstrated glutathione *S*-transferase placental form (GST-P) positive foci, as previously described[25]. GST-P positive foci larger than 0.2 mm in diameter and the total areas of the liver sections examined were quantitated using a video image processor (SPICCA-II, Nippon Avionics, Tokyo, Japan) and the data expressed as numbers and areas (mm^2) per unit area of the liver section (cm^2).

Statistical analysis

The significance of intergroup differences in numerical data obtained for body and organ weights was assessed using the two-tailed Student's t-test. Insufficient homogeneity of variance was corrected with respect to the degrees of freedom according to the method of Welch. The significance of differences in the incidences of histopathological findings between treated and control groups was evaluated using Fisher's exact probability test.

Results

No post-initiation treatment-related clinical signs or mortalities were noted in any of the groups in the current experiment. Eight rats were found dead in the course of study, one in group 1, three in group 2, one in group 3, two in group 4 and one in group 5, and the deaths were all considered to have been caused by the DMBDD treatment.

The average body weights of rats in the DMBDD treated groups were significantly less than in the non-DMBDD initiated groups, throughout the study period. After DMBDD initiation, 30% DHA-TG was associated with retardation of body weight increase from week 7. The body weights in the other DMBDD treated groups were not

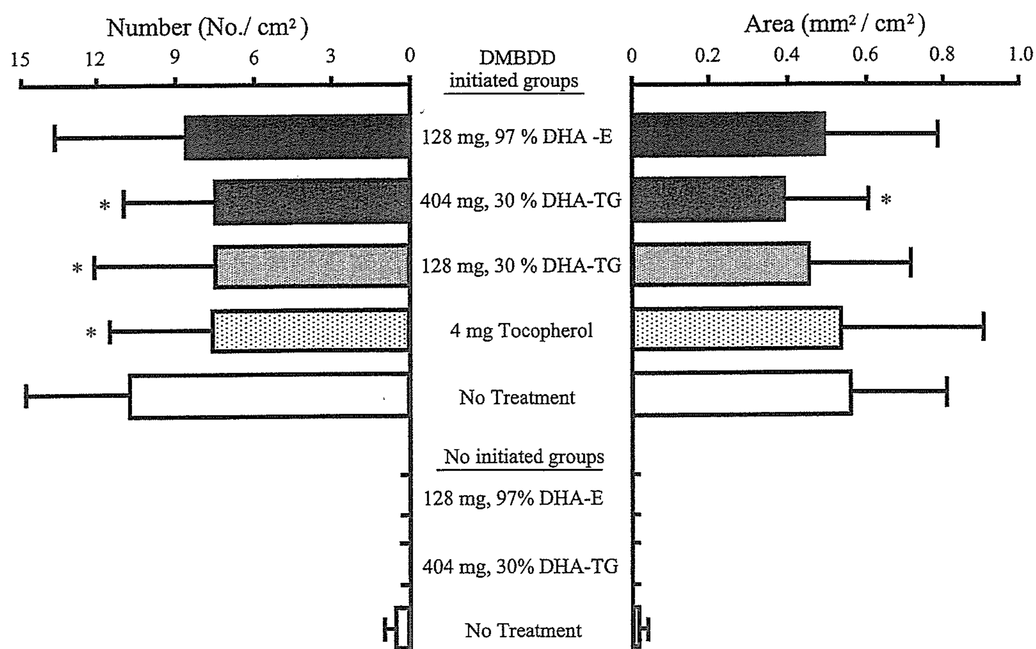

Fig. 2. Areas and numbers of GST-P positive foci in rat livers. * P<0.05 versus DMBDD initiated no treatment group.

Table 3. Number of ACF in Rats Treated with and without DHA during the Post-Initiation Stage

Groups	DMBDD	Treatment	Effective no. of rats	ACF / Colon < 4 crypts	ACF / Colon 4 crypts≤	ACF / Colon Total	AC / Focus
1	+	128 mg 97% DHA-E	9	27.1 ± 6.9	6.2 ± 3.9	33.3 ± 9.7	2.5 ± 0.3
2	+	404 mg 30% DHA-TG	9	27.0 ± 14.3	6.2 ± 6.1	33.2 ± 18.3	2.3 ± 0.4
3	+	128 mg 30% DHA-TG	9	26.6 ± 7.5	7.9 ± 4.6	34.4 ± 11.6	2.5 ± 0.4
4	+	4 mg Tocopherol	9	25.9 ± 16.9	5.2 ± 3.8	31.1 ± 19.3	2.4 ± 0.3
5	+	no treatment	10	26.8 ± 10.1	8.2 ± 5.7	35.0 ± 13.5	2.7 ± 0.4
6	–	128 mg 97% DHA-E	5	0.3 ± 0.5	0	0.2 ± 0.5	0.4 ± 0.9
7	–	404 mg 30% DHA-TG	5	0.3 ± 0.5	0.2 ± 0.5	0.4 ± 0.6	1.4 ± 0.2
8	–	no treatment	5	0.3 ± 0.5	0	0.2 ± 0.5	0.2 ± 0.5

AC: aberrant crypts.

significantly changed.

A significant increase in relative liver weight and a tendency to increase in relative kidney weights were noted in group 2 (Table 2).

Quantitative analysis of GST-P positive foci (Fig. 2) showed the numbers and areas were significantly decreased by the 404 mg/ml 30% DHA-TG treatment. The numbers were also suppressed by 128 mg/ml 30% DHA-TG and tocopherol alone.

No significant difference was observed in ACF between DHA and/or tocopherol treatment groups and the DMBDD alone group (Table 3).

Histopathological examination revealed hyperplastic and neoplastic lesions in various organs/tissues in the rats initiated with the five carcinogens (Tables 4, 5). However, no DHA treatment-related alteration in their incidences was evident. No proliferative lesions were noted in any of the rats given DHA and tocopherol without DMBDD treatment.

Discussion

The present investigation of the modifying potential of DHA in a rat medium-term multi-organ carcinogenesis model found no modifying effects on lesion development in any organ. Decreases of number and/or area of GST-P positive foci in the liver given 404 mg and 128 mg 30% DHA-TG were demonstrated, but similar results were obtained with tocopherol alone, so the latter was considered responsible, in line with its reported inhibitory potential[26,27].

The effect of dietary sardine oil including 28.5% DHA on rat hepatocarcinogenesis was examined with administration in the initiation and post-initiation period[28]. The sardine oil inhibited the number of DEN-induced GST-P positive foci when administered in the initiation period, but enhanced the area of GST-P positive foci when administered in the post-initiation period. However, in another study, fish oil inhibited AOM-induced GST-P positive foci in the post-

Table 4. Incidences of Neoplastic Lesions in the Large and Small Intestines

Groups	DMBDD	Treatment	Effective no. of rats	Small intestine		Large intestine	
				Adenoma	Adenocarcinoma	Adenoma	Adenocarcinoma
1	+	128 mg 97% DHA-E	20	0	1 (5)	1 (5)	1 (5)
2	+	404 mg 30% DHA-TG	20	2 (10)	4 (20)	0	1 (5)
3	+	128 mg 30% DHA-TG	20	1 (5)	1 (5)	2 (10)	1 (5)
4	+	4 mg Tocopherol	20	1 (5)	1 (5)	1 (5)	1 (5)
5	+	no treatment	20	2 (10)	2 (10)	1 (5)	1 (5)
6	–	128 mg 97% DHA-E	10	0	0	0	0
7	–	404 mg 30% DHA-TG	10	0	0	0	0
8	–	no treatment	10	0	0	0	0

Table 5. Incidences of Preneoplastic and Neoplastic Lesions in Other Organs in DMBDD Treated Groups

Organ / Findings		DMBDD treatment				
		128 mg 97% DHA-E	404 mg 30% DHA-TG	128 mg 30% DHA-TG	4 mg Tocopherol	No treatment
No. of rats examined		20	20	20	20	20
Spleen:	Hemangioma	0	0	0	0	1 (5)
Thyroids:	Follicular cell hyperplasia	13 (65)	17 (85)	10 (50)	12 (60)	10 (50)
	Follicular cell adenoma	4 (20)	10 (50)	9 (45)	5 (25)	6 (30)
	Follicular cell carcinoma	5 (25)	7 (35)	6 (30)	5 (25)	5 (25)
Nasal cavity:	Hyperplasia	17 (85)	19 (95)	17 (85)	20 (100)	20 (100)
	Adenoma	2 (10)	0	0	1 (5)	0
Lung:	Alveolar hyperplasia	20 (100)	20 (100)	20 (100)	20 (100)	20 (100)
	Adenoma	8 (40)	6 (30)	8 (40)	10 (50)	8 (40)
	Adenocarcinoma	1 (5)	4 (20)	2 (10)	3 (15)	4 (20)
Tongue:	Squamous cell hyperplasia	0	0	2 (10)	1 (5)	0
	Papilloma	0	0	0	1 (5)	0
Esophagus:	Squamous cell hyperplasia	18 (90)	17 (85)	19 (95)	20 (100)	17 (85)
	Papilloma	0	2 (10)	0	0	1 (5)
Stomach:	Squamous cell hyperplasia	10 (50)	8 (40)	12 (60)	12 (60)	13 (65)
	Squamous cell papilloma	3 (15)	1 (5)	2 (10)	0	3 (15)
	Squamous cell carcinoma	0	1 (5)	0	1 (5)	0
Liver:	Hepatocellular adenoma	3 (15)	1 (5)	2 (10)	1 (5)	5 (25)
	Hepatocellular carcinoma	0	0	0	1 (5)	0
Kidneys:	Atypical tubules	11 (55)	13 (65)	7 (35)	10 (50)	9 (45)
	Renal cell hyperplasia	0	0	1 (5)	0	0
	Transitional cell hyperplasia	6 (30)	8 (40)	4 (20)	4 (20)	8 (40)
	Renal cell adenoma	1 (5)	1 (5)	3 (15)	1 (5)	1 (5)
	Nephroblastoma	5 (25)	7 (35)	6 (30)	4 (20)	10 (50)
	Transitional cell carcinoma	0	3 (15)	0	0	1 (5)
Urinary bladder:	Simple hyperplasia	12 (60)	12 (60)	14 (70)	13 (65)	11 (55)
	PN hyperplasia	4 (20)	2 (10)	4 (20)	3 (15)	3 (15)
	Papilloma	0	0	0	0	1 (5)
	Transitional cell carcinoma	1 (5)	1 (5)	0	1 (5)	0
Other site:	Histiocytic sarcoma	0	0	0	1 (5)	0
	Leiomyosarcoma	0	0	0	1 (5)	1 (5)
	Malignant lymphoma/ leukemia	1 (5)	1 (5)	1 (5)	1 (5)	0

initiation stage[29]. These results suggest that the effects of fish oil appear to be dependent on the types of carcinogens. In the present study, DHA did not enhance hepatocarcinogenesis initiated with five carcinogens.

Some previous studies indicated the chemopreventive effect of DHA on colon[1–4], mammary glands[6] and pancreas carcinogenesis[5] in rats. DHA exerted significant inhibitory effects on implanted tumor growth and metastasis to the lungs in a subcutaneously implanted and highly metastatic colon carcinoma model[30]. However, no chemoprevention was observed for rat colon and other organ carcinogenesis with DHA treatment in the present study. The reason for the discrepancy with the many previous studies which showed chemopreventive effects on colon carcinogenesis and ACF development[1–4,27,31,32], may be due to the different number of treatment times per week. DHA was injected five times a

week or administered in diet continuously in the other chemopreventive studies, but injected three times a week in this study, according to the clinical trial study[7].

In the multi-organ model (DMBDD model)[20,21,23,33] incidences of colon tumor development have been reported to range from 10 to 80%, therefore the figure of 10% achieved in the present study was relatively low. Thus, one reason for the lack of obvious influence of DHA could have been due to weak initiation.

Recently, different results regarding the chemopreventive effect of DHA-E in diet using the same model were published by an other group[33]. They showed an inhibitory effect on carcinogenesis in the small intestine, large intestine and lung by DHA. They used synthetic diet (modified AIN-93) as basal diet for the experiment, but we used a conventional diet (Oriental MF), this may have been the cause of the different results.

DHA has been reported as an useful chemopreventive agent in many rodent studies[1–6]. However, in a long-term trial using concentrated DHA in fish oil capsules containing about 30% DHA in triglyceride form, for patients in a high-risk group for colorectal cancer, three patients with FAP developed cancers, one endometrial, one colon and one lung[7]. During the trial, no marked increase or decrease in the number of polyps was observed.

In the present experiment, no promotion activity of either DHA-E or DHA-TG was found in any organ including the large intestine. The reason for the tumor development seen in the clinical trial study with DHA-TG treatment could not therefore be clarified in the present study.

Acknowledgements: This work was supported in part by a Grant-in-Aid for Cancer Research from the Ministry of Health, Labour and Welfare, Japan, a grant from the Society for Promotion of Pathology of Nagoya, and a grant from Nippon Suisan Kaisha, Ltd., Japan.

References

1. Takahashi M, Minamoto T, Yamashita N, Yazawa K, Sugimura T, and Esumi H. Reduction in formation and growth of 1,2-dimethylhydrazine-induced aberrant crypt foci in rat colon by docosahexaenoic acid. Cancer Res. **53**: 2786–2789. 1993.
2. Takahashi M, Minamoto T, Yamashita N, Kato T, Yazawa K, and Esumi H. Effect of docosahexaenoic acid on azoxymethane-induced colon carcinogenesis in rats. Cancer Lett. **83**: 177–184. 1994.
3. Takahashi M, Fukutake M, Isoi T, Fukuda K, Sato H, Yazawa K, Sugimura T, and Wakabayashi K. Suppression of azoxymethane-induced rat colon carcinoma development by a fish oil component, docosahexaenoic acid (DHA). Carcinogenesis. **18**: 1337–1342. 1997.
4. Takahashi M, Totsuka Y, Masuda M, Fukuda K, Oguri A, Yazawa K, Sugimura T, and Wakabayashi K. Reduction in formation of 2-amino-1-methyl-6-phenylimidazo[*4,5-b*]pyridine (PhIP) -induced aberrant crypt foci in the rat colon by docosahexaenoic acid (DHA). Carcinogenesis. **18**: 1937–1941. 1997.
5. Appel MJ and Wouterson RA. Modulation of growth and cell turnover of preneoplastic lesion and of prostaglandin levels in rat pancreas by dietary fish oil. Carcinogenesis. **15**: 2107–2112. 1994.
6. Noguchi M, Minami M, Yagasaki R, Kinoshita K, Earashi M, Kitagawa H, Taniya T, and Miyazaki I. Chemoprevention of DMBA-induced mammary carcinogenesis in rats by low-dose EPA and DHA. Br J Cancer. **75**: 348–353. 1997.
7. Akedo I, Ishikawa H, Nakamura T, Kimura K, Takeyama I, Suzuki T, Kameyama M, Sato S, Nakamura T, Matsuzawa Y, Kakizoe T, and Otani T. Three cases with familial adenomatous polyposis diagnosed as having malignant lesions in the course of a long-term trial using docosahexaenoic acid (DHA)-concentrated fish oil capsules. Jpn J Clin Oncol. **28**: 762–765. 1998.
8. Hirose M, Tanaka H, Takahashi S, Futakuchi M, Fukushima S, and Ito N. Effects of sodium nitrite and catechol, 3-methoxycatechol, or butylated hydroxyanisole in combination in a rat multiorgan carcinogenesis model. Cancer Res. **53**: 22–37. 1993.
9. Imaida K, Fukushima S, Shirai T, Ohtani M, Nakanishi K, and Ito N. Promoting activities of butylated hydroxyanisole and butylated hydroxytoluene on 2 stage urinary bladder carcinogenesis and inhibition of γ-glutamyl transpeptidase-positive foci development in the liver of rats. Carcinogenesis. **4**: 895–899. 1983.
10. Wattenberg LW and Sparnins VL. Inhibitory effects of butylated hydroxyanisole on methylazoxymethanol acetate-induced neoplasia of the large intestine and on nicotinamide adenine dinucleotide-dependent alcohol dehydrogenase activity in mice. J Natl Cancer Inst. **63**: 219–222. 1979.
11. Ito N, Imaida K, Tsuda H, Shibata M, Aoki T, deCamargo JLV, and Fukushima S. Wide-spectrum initiation models: possible application to medium-term multiple organ bioassays for carcinogenesis modifiers. Jpn J Cancer Res. **79**: 413–417. 1988.
12. Thamavit W, Fukushima S, Kurata Y, Asamoto M, and Ito N. Modification by sodium L-ascorbate, butylated hydroxytoluene, phenobarbital and pepleomycin of lesion development in a wide-spectrum initiation rat model. Cancer Lett. **45**: 93–101. 1989.
13. Shibata M-A, Fukushima S, Takahashi S, Hasegawa R, and Ito N. Enhancing effects of sodium phenobarbital and *N*, *N*-dibutylnitrosamine on tumor development in a rat wide-spectrum organ carcinogenesis model. Carcinogenesis. **11**: 1027–1031. 1990.
14. Fukushima S, Hagiwara A, Hirose M, Yamaguchi S, Tiwawech D, and Ito N. Modifying effects of various chemicals on preneoplastic and neoplastic lesion development in a wide-spectrum organ carcinogenesis model using F344 rats. Jpn J Cancer Res. **82**: 642–649. 1991.
15. Takahashi S, Hasegawa R, Masui T, Mizoguchi M, Fukushima S, and Ito N. Establishment of a multi-organ carcinogenesis bioassay using rats treated with a combination of five different carcinogens. J Toxicol Pathol. **5**: 151–156. 1992.
16. Fukushima S, Shibata M-A, Hirose M, Kato T, Tatematsu M, and Ito N. Organ-specific modification of tumor development by low-dose combinations of agents in a rat

wide-spectrum carcinogenesis model. Jpn J Cancer Res. **82**: 784–792. 1991.

17. Hirose M, Hoshiya T, Akagi K, Takahashi S, Hara Y, and Ito N. Effects of green tea catechins in a rat multi-organ carcinogenesis model. Carcinogenesis. **14**: 1549–1553. 1993.
18. Hagiwara A, Tanaka H, Imaida K, Tamano S, Fukushima S, and Ito N. Correlation between medium-term multi-organ carcinogenesis bioassay data and long-term observation results in rats. Jpn J Cancer Res. **84**: 237–245. 1993.
19. Takahashi S, Hakoi K, Yada H, Hirose M, Ito N, and Fukushima S. Enhancing effects of diallyl sulfide on hepatocarcinogenesis and inhibitory actions of the related diallyl disulfide on colon and renal carcinogenesis in rats. Carcinogenesis. **13**: 1513–1518. 1992.
20. Taniyama T, Wanibuchi H, Salim EI, Yano Y, Otani S, Nishizawa Y, Morii H, and Fukushima S. Chemopreventive effect of 24*R*,25-dihydroxyvitamin D3 in *N,N'*-dimethylhydrazine-induced rat colon carcinogenesis. Carcinogenesis. **21**: 173–178. 2000.
21. Shibata M-A, Hasegawa R, Imaida K, Hagiwara A, Ogawa K, Hirose M, Ito N, and Shirai T. Chemoprevention by dehydroepiandrosterone and indomethacin in a rat multiorgan carcinogenesis model. Cancer Res. **55**: 4870–4874. 1995.
22. Hirose M, Takesada Y, Tanaka H, Tamano S, Kato T, and Shirai T. Carcinogenicity of antioxidants BHA, caffeic acid, sesamol, 4-methoxyphenol and catechol at low doses, either alone or in combination, and modulation of their effects in a rat medium-term multi-organ carcinogenesis bioassay model. Carcinogenesis. **19**: 207–212. 1997.
23. Kimura J, Takahashi S, Ogiso T, Yoshida Y, Akagi K, Hasegawa R, Kurata M, Hirose M, and Shirai T. Lack of chemoprevention effects of the monoterpene d-limonene in a rat multi-organ carcinogenesis model. Jpn J Cancer Res. **87**: 589–594. 1996.
24. Bird RP. Observation and quantification of aberrant crypts in the murine colon treated with a colon carcinogen: preliminary findings. Cancer Lett. **37**: 147–151. 1987.
25. Tatematsu M, Mera Y, Ito N, Satoh K, and Sato K. Relative merits of immunohistochemical demonstrations of placental, A, B and C forms of glutathione S-transferase as markers of altered foci during liver carcinogenesis in rats. Carcinogenesis. **6**: 1621–1626. 1985.
26. Tsuda H, Uehara N, Iwahori Y, Asamoto M, Iigo M, Nagao M, Matsumoto K, Ito M, and Hirono I. Chemopreventive effects of β-carotene, α-tocopherol and five naturally occurring antioxidants on initiation of hepatocarcinogenesis by 2-amino-3-methylimidazo[*4,5-f*]quinoline in the rat. Jpn J Cancer Res. **85**: 1214–1219. 1994.
27. Tsuda H, Iwahori Y, Asamoto M, Baba-Toriyama H, Hori T, Kim DJ, Uehara N, Iigo M, Takasuka N, Murakoshi M, Nishino H, Kakizoe T, Araki E, and Yazawa K. Demonstration of organotropic effects of chemopreventive agents in multiorgan carcinogenesis models. IARC Sci Publ. **139**: 143–150. 1996.
28. Rahman KMW, Sugie S, Okamoto K, Watanabe T, Tanaka T, and Mori H. Modulating effects of diets high in ω-3 and ω-6 fatty acids in initiation and postinitiation stages of diethylnitrosamine-induced hepatocarcinogenesis in rats. Jpn J Cancer Res. **90**: 31–39. 1999.
29. Sugie S, Okamoto K, Tanaka T, Mori H, Reddy BS, and Satoh K. Effect of fish oil on the development of AOM-induced glutathione S-transferase placental form positive hepatocellular foci in male F344 rats. Nutr Cancer. **24**: 187–195. 1995.
30. Iigo M, Nakagawa T, Ishikawa C, Iwahori Y, Asamoto M, Yazawa K, Araki E, and Tsuda H. Inhibitory effects of docosahexaenoic acid on colon carcinoma 26 metastatisis to the lung. Br J Cancer. **75**: 650–655. 1997.
31. Reddy BS, Burill C, and Rigotty J. Effects of diets high in ω-3 and ω-6 fatty acid on initiation and postinitiation stages of colon carcinogenesis. Cancer Res. **51**: 487–491. 1991.
32. Paulsen JE, Stamm T, and Alexander J. A fish oil-derived concentrate enriched in eicosapentaenoic acid and docosahexaenoic acid as ethyl esters inhibits the formation and growth of aberrant crypt foci in rat colon. Pharmacol Toxicol. **82**: 28–33. 1998.
33. Toriyama-Baba H, Iigo M, Asamoto M, Iwahori Y, Park CB, Han BS, Takasuka N, Kakizoe T, Ishikawa C, Yazawa K, Araki E, and Tsuda H. Organotropic chemopreventive effects of n-3 unsaturated fatty acid in a rat multi-organ carcinogenesis model. Jpn J Cancer Res. **92**: 1175–1183. 2002.

British Journal of Cancer (2005) 92, 1240–1246
© 2005 Cancer Research UK All rights reserved 0007–0920/05 $30.00
www.bjcancer.com

Translational Therapeutics

NK105, a paclitaxel-incorporating micellar nanoparticle formulation, can extend *in vivo* antitumour activity and reduce the neurotoxicity of paclitaxel

T Hamaguchi[1], Y Matsumura*[,1,2], M Suzuki[3], K Shimizu[3], R Goda[3], I Nakamura[3], I Nakatomi[4], M Yokoyama[5], K Kataoka[6] and T Kakizoe[7]

[1]*Department of Medicine, President of National Cancer Center, 5-1-1 Tsukiji, Chuo-ku, Tokyo 104-0045, Japan;* [2]*Investigative Treatment Division, National Cancer Center Research Institute East, 6-5-1 Kashiwanoha, Kashiwa, Chiba 277-8577, Japan;* [3]*Pharmaceuticals Group, Research & Development Division, Nippon Kayaku Co., Ltd, 3-31-12 Shimo, Kita-ku, Tokyo 115-8588, Japan;* [4]*NanoCarrier Co., Ltd, Tokatsu Techno Plaza, 5-4-6 Kashiwanoha, Kashiwa, Chiba 277-0882, Japan;* [5]*Kanagawa Academy of Science and Technology, KSP Bldg., East 404, 3-2-1 Sakado, Takatsu-ku, Kawasaki, Kanagawa 213-0012, Japan;* [6]*Department of Materials Engineering, Graduate School of Engineering, The University of Tokyo, 7-3-1 Hongo, Bunkyo-ku, Tokyo 113-8656, Japan;* [7]*President of National Cancer Center, 5-1-1 Tsukiji, Chuo-ku, Tokyo 104-0045, Japan*

Paclitaxel (PTX) is one of the most effective anticancer agents. In clinical practice, however, high incidences of adverse reactions of the drug, for example, neurotoxicity, myelosuppression, and allergic reactions, have been reported. NK105, a micellar nanoparticle formulation, was developed to overcome these problems and to enhance the antitumour activity of PTX. Via the self-association process, PTX was incorporated into the inner core of the micelle system by physical entrapment through hydrophobic interactions between the drug and the well-designed block copolymers for PTX. NK105 was compared with free PTX with respect to their *in vitro* cytotoxicity, *in vivo* antitumour activity, pharmacokinetics, pharmacodynamics, and neurotoxicity. Consequently, the plasma area under the curve (AUC) values were approximately 90-fold higher for NK105 than for free PTX because the leakage of PTX from normal blood vessels was minimal and its capture by the reticuloendothelial system minimised. Thus, the tumour AUC value was 25-fold higher for NK105 than for free PTX. NK105 showed significantly potent antitumour activity on a human colorectal cancer cell line HT-29 xenograft as compared with PTX ($P<0.001$) because the enhanced accumulation of the drug in the tumour has occurred, probably followed by its effective and sustained release from micellar nanoparticles. Neurotoxicity was significantly weaker with NK105 than with free PTX. The neurotoxicity of PTX was attenuated by NK105, which was demonstrated by both histopathological ($P<0.001$) and physiological ($P<0.05$) methods for the first time. The present study suggests that NK105 warrants a clinical trial for patients with metastatic solid tumours.
British Journal of Cancer (2005) **92,** 1240–1246. doi:10.1038/sj.bjc.6602479 www.bjcancer.com
Published online 22 March 2005
© 2005 Cancer Research UK

Keywords: NK105; paclitaxel; polymer micelles; DDS; EPR effect

Paclitaxel (PTX) is one of the most useful anticancer agents known for various cancers including ovarian, breast, and lung cancers (Carney, 1996; Khayat *et al*, 2000). However, PTX has serious adverse effects, for example, neutropenia and peripheral sensory neuropathy. In addition, anaphylaxis and other severe hypersensitive reactions have been reported to develop in 2–4% of patients receiving the drug even after premedication with antiallergic agents; these adverse reactions have been attributed to the mixture of Cremophor EL and ethanol, which was used to solubilise PTX (Weiss *et al*, 1990; Rowinsky and Donehower, 1995). Of the adverse reactions, neutropenia can be prevented or managed effectively by administering a granulocyte colony-stimulating factor. On the other hand, there are no effective therapies to prevent or reduce nerve damage, which is associated with peripheral neuropathy caused by PTX; therefore, neurotoxicity constitutes a significant dose-limiting toxicity of the drug (Rowinsky *et al*, 1993; Wasserheit *et al*, 1996).

The above problems of PTX have been attributed to its low therapeutic indices and limited efficacy due to the nonselective nature of its therapeutic targets and its inability to accumulate selectively in cancer tissue. Therefore, there is an urgent need to develop modalities by which cytotoxic drugs can selectively target tumour tissue and effectively act on cancer cells in the scene. The roles of drug delivery systems (DDSs) have drawn attention in this context. Drug delivery systems are based on two main principles: active and passive targetings. The former refers to the development of monoclonal antibodies directed against tumour-related molecules that allow targeting of the tumour because of specific binding between the antibody and its antigen. However, the application of

*Correspondence: Dr Y Matsumura, Investigative Treatment Division, National Cancer Center Research Institute East, 6-5-1 Kashiwanoha, Kashiwa, Chiba 277-8577, Japan; E-mail: yhmatsum@east.ncc.go.jp
Received 27 October 2004; revised 26 January 2005; accepted 31 January 2005; published online 22 March 2005

DDSs using monoclonal antibodies is restricted to tumours expressing high levels of related antigens.

Passive targeting is based on the so-called enhanced permeability and retention (EPR) effect (Matsumura and Maeda, 1986; Maeda *et al*, 2000). The EPR effect consists in the pathophysiological characteristics of solid tumour tissue: hypervascularity, incomplete vascular architecture, secretion of vascular permeability factors stimulating extravasation within cancer tissue, and absence of effective lymphatic drainage from tumours that impedes the efficient clearance of macromolecules accumulated in solid tumour tissues.

Several techniques to maximally use the EPR effect have been developed, that is, modification of drug structures and development of drug carriers. The first micelle-forming polymeric drug developed was polyethylene glycol (PEG)-polyaspartate block copolymer conjugated with doxorubicin (DXR) (Yokoyama *et al*, 1990; Yokoyama *et al*, 1991; Kataoka *et al*, 1993). PEG constituted the outer shell of the micelle, which conferred a stealth property on the drug that allowed the micellar drug preparations to be less avidly taken up by the reticuloendothelial system (RES) and to be retained in the circulation for a longer time. Prolonged circulation time and the ability of polymeric micelles to extravasate through the leaky tumour vasculature were expected to result in the accumulation of DXR in tumour tissue due to the EPR effect (Kwon *et al*, 1994; Yokoyama *et al*, 1999). A clinical trail of micellar DXR, NK911, is now underway (Nakanishi *et al*, 2001; Hamaguchi *et al*, 2003). Recently, we succeeded in constructing NK105, a polymeric micelle carrier system for PTX, which conferred on PTX a passive targeting ability based on the EPR effect. In the present paper, we describe the details and characteristics of NK105. We also discuss differences between NK105 and other DDS formulations containing PTX.

MATERIALS AND METHODS

Materials

PTX was purchased from Mercian Corp. (Tokyo, Japan). All other chemicals were of reagent grade. Following cell lines, MKN-45, MKN-28, HT-29, DLD-1, HCT116, TE-1, TE-8, PC-14, PC-14/TXT, H460, MCAS, OVCAR-3, AsPC-1, PAN-9, PAN-3, and MCF-7 cells were purchased from American Type Culture Collection. Colon 26 cells were dispensed from the Japan Foundation for Cancer Research (Tokyo, Japan). Female BALB/c *nu/nu* mice were purchased from SLC (Shizuoka, Japan). Female CDF1 mice and IGS rats were purchased from Charles River Japan Inc. (Kanagawa, Japan).

All animal procedures were performed in compliance with the guidelines for the care and use of experimental animals, which had been drawn up by the Committee for Animal Experimentation of the National Cancer Center; these guidelines meet the ethical standards required by law and also comply with the guidelines for the use of experimental animals in Japan.

NK105, a PTX-incorporating micellar nanoparticle formulation

NK105 is a PTX-incorporating 'core-shell-type' polymeric micellar nanoparticle formulation. Polymeric micellar particles were formed by facilitating the self-association of amphiphilic block copolymers in an aqueous medium. Novel amphiphilic block copolymers, namely NK105 polymers, were designed for PTX entrapment. NK105 polymers were constructed using PEG as the hydrophilic segment and modified polyaspartate as the hydrophobic segment. Carboxylic groups of polyaspartate block were modified with 4-phenyl-1-butanol by esterification reaction, consequently the half of the groups were converted to 4-phenyl-1-butanolate. Via the self-association process, PTX was incorporated into the inner core of the micelle system by physical entrapment through hydrophobic interactions between the drug and specifically well-designed block copolymers for PTX.

Pharmacokinetics and pharmacodynamics of PTX and NK105

Colon 26 tumour-bearing CDF1 mice aged 8 weeks were given intravenously (i.v.) via the tail vein PTX 50 and 100 mg kg^{-1} or NK105 at corresponding PTX-equivalent doses. Mice were killed at 5 and 30 min, as well as 2, 6, 24, and 72 h after injection. Blood was collected, and tumours were removed; plasma and tumours obtained were then stored at −20°C until the analysis. Each time point for collection represented three samples from three different mice. PTX was extracted from plasma obtained by deproteinisation using acetonitrile, followed by liquid–liquid extraction with *t*-butylmethylether. Tumours obtained were homogenised in 0.5% acetic acid, and the resultant homogenate was deproteinised and extracted according to the same method as that used for plasma. The blood and tumour extracts were analysed for PTX by liquid chromatography/tandem mass spectrometry. Reversed-phase column-switching chromatography was conducted using an ODS column and detection was enabled by electrospray ionisation of positive mode. The mean plasma and tumour concentrations of PTX at each sampling point were calculated for both PTX and NK105. Pharmacokinetic modelling was completed using a WinNonlin Standard software version 3.1 (Pharsight Corp., California, USA).

In vitro cytotoxicity

Various human cancer cell lines were evaluated in the present study. The cell lines were maintained in monolayer cultures in Dulbecco's modified Eagle's medium containing 10% (v v^{-1}) foetal calf serum and 600 mg l^{-1} glutamine. WST-8 Cell Counting Kit-8 (Dojindo, Kumamoto, Japan) was used for the cell proliferation assay. In all, 2000 cells of each cell line in 90 μl of culture medium were plated in 96-well plates and were then incubated for 24 h at 37°C. Serial dilutions of PTX or NK105 in a volume of 10 μl were added, and the cells were incubated for 48 or 72 h. All data were expressed as mean $\pm$ s.e. of triplicate cultures. The data were then plotted as a percentage of the data from the control cultures, which were treated identically to the experimental cultures, except that no drug was added.

Evaluation of the antitumour activity of PTX and NK105

The antitumour activity of PTX and NK105 was evaluated using nude mice implanted with a human colonic cancer cell line, HT-29. One million tumour cells of HT-29 were inoculated at a subcutaneous (s.c.) site on the back skin of BALB/c female nude mice aged 6 weeks. When tumour size reached approximately 5–8 mm in diameter, mice were randomly allocated to the PTX administration group, NK105 administration group, and control administration group, each of which was made up of five animals. Each treatment was carried out as follows: free PTX group was administered at a dose of 25, 50, or 100 mg kg^{-1}; NK105 group was with same PTX-equivalent doses; and in control group, animals were given saline. Mice were administered a single i.v. injection of PTX or NK105 weekly for 3 weeks. The antitumour activity of PTX and NK105 was evaluated by measuring tumour size ($a \times b$, where a is the major diameter and b is the minor diameter) at various time points after injection. Changes in body weight were also monitored for mice, which were used in the present study.

© 2005 Cancer Research UK

Evaluation of neurotoxicity

The severity of neurotoxicity was assessed both electrophysiologically and histologically. Under intraperitoneal ketamine anaesthesia (40 mg kg^{-1}), rats were given a single i.v. injection of PTX (7.5 mg kg^{-1}), NK105 (a PTX-equivalent dose of 7.5 mg kg^{-1}), or 5% glucose weekly for 6 weeks. All the solutions were administered through the jugular vein exposed via a small incision in the neck. Electrophysiological measurements were conducted 1 day before the first dosing and on day 6 after the final dosing. For electrophysiological recording, rats were anaesthetised by the intraperitoneal injection of pentobarbital 40 mg kg^{-1}. Electrical stimuli were given peripherally, and caudal sensory nerve action potentials (caudal SNAPs) were recorded centrally from the tail. The amplitude of each waveform was calculated by measuring the caudal SNAP from the top peak to the bottom peak. Variations in the amplitude after the 6th weekly administration of the solutions were determined.

For light microscopy, rats were killed after electrophysiological recordings. Subsequently, a segment of the sciatic nerve was carefully removed, and embedded in paraffin. Sections (2 μm thick) were stained with haematoxylin and eosin (H & E) before examination under light microscopy to evaluate the degenerative changes of myelinated nerve fibres.

Statistical analysis

The data of therapeutic efficacy was expressed as mean $\pm$ s.e.m. The statistical significance of differences in therapeutic efficacy between two administration groups was calculated by means of repeated measures (analysis of variance). The statistical significance of the differences in neurotoxic activity between two administration groups was calculated using the Student's t-test on the closed testing procedure. The histopathological impairment was scored in five grades. The statistical significance of the differences in histopathological impairment between two administration groups was calculated using the Wilcoxon's rank-sum test on the closed testing procedure. All data were calculated with software StatView, version 5 (ABACUS Concepts, Berkeley, CA, USA). A value of $P<0.05$ was considered statistically significant.

RESULTS

Preparation and characterisation of NK105

To construct NK105 micellar nanoparticles (Figure 1A), block copolymers consisting of PEG and polyaspartate, the so-called PEG polyaspartate described previously (9, 11, 13, 14), were used. PTX was incorporated into polymeric micelles formed by physical entrapment utilising hydrophobic interactions between PTX and the block copolymer polyaspartate chain. After screening of many candidate substances, 4-phenyl-1-butanol was employed for the chemical modification of the polyaspartate block to increase its hydrophobicity. Treating with a condensing agent, 1,3-diisopropylcarbodiimide, the half of carboxyl groups on the polyaspartate, was esterified with 4-phenyl-1-butanol. Molecular weight of the polymers was determined to be approximately 20 000 (PEG block: 12 000; modified polyaspartate block: 8000). NK105 was prepared by facilitating the self-association of NK105 polymers and PTX. NK105 was obtained as a freeze-dried formulation and contained ca. 23% (w w^{-1}) of PTX, as determined by reversed-phase liquid chromatography using an ODS column with mobile phase consisting of acetonitrile and water (9:11, v v^{-1}) and detection of ultraviolet absorbance at 227 nm. Finally, NK105, a PTX-incorporating polymeric micellar nanoparticle formulation with a single and narrow size distribution, was obtained. The weight-average diameter of the nanoparticles was approximately 85 nm ranging from 20 to 430 nm (Figure 1B).

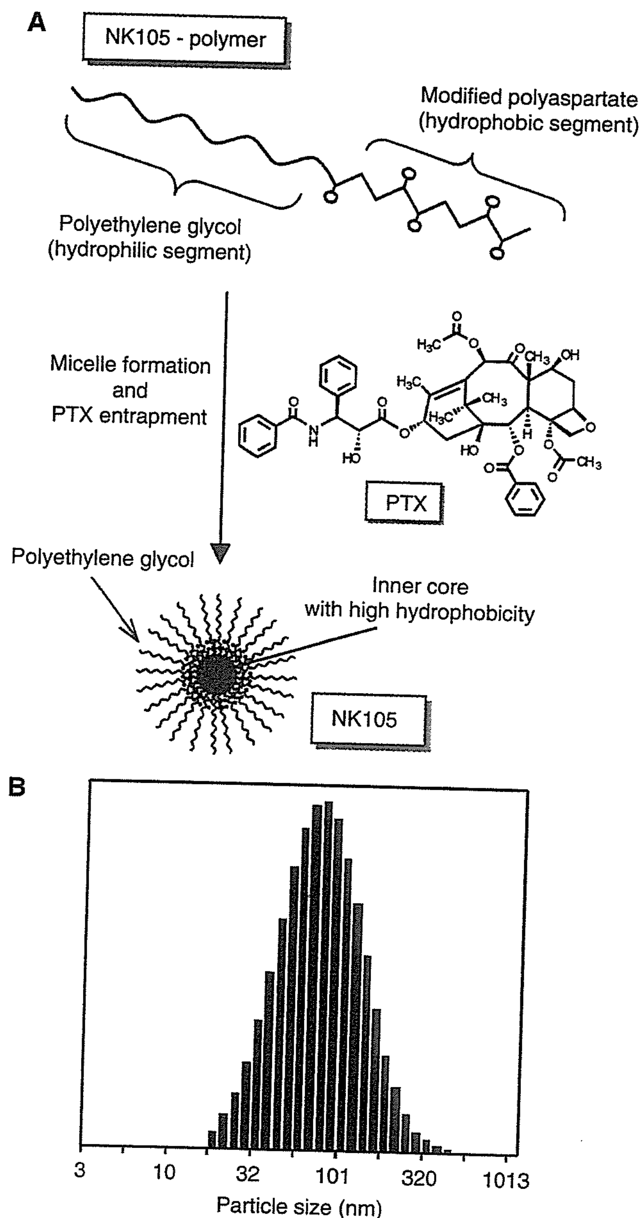

Figure 1 Preparation and characterisation of NK105. (**A**) The micellar structure of NK105 PTX was incorporated into the inner core of the micelle. (**B**) The size distribution of NK105 measured by the dynamic light scattering method. The mean diameter of an NK105 micelle was 85 nm.

Pharmacokinetics and pharmacodynamics of NK105

Colon 26-bearing CDF1 mice were given a single i.v. injection of PTX 50 or 100 mg kg^{-1}, or of NK105 at an equivalent dose of PTX. Subsequently, the time-course changes in the plasma and tumour levels of PTX were determined in the PTX and NK105 administration groups (Figure 2); furthermore, the pharmacokinetic parameters of each group were also determined (Table 1). NK105 exhibited slower clearance from the plasma than PTX, while NK105 was present in the plasma for up to 72 h after injection; PTX was not detected after 24 h or later of injection. The plasma concentration at 5 min ($C_{5\,min}$) and the area under the curve (AUC) of NK105 were 11–20-fold and 50–86-fold higher for NK105 than for PTX, respectively. Furthermore, the half-life at the terminal phase ($t_{1/2}z$) was 4–6 times longer for NK105 than for

© 2005 Cancer Research UK

PTX. The maximum concentration (C_{max}) and AUC of NK105 in Colon 26 tumours were approximately 3 and 25 times higher for NK105 than for PTX, respectively. NK105 continued to accumulate in the tumours until 72 h after injection. The tumour PTX concentration was higher than 10 $\mu g\,g^{-1}$ even at 72 h after the i.v. injection of NK105 50 and 100 $mg\,kg^{-1}$. On the contrary, the tumour PTX concentrations at 72 h after the i.v. administration of free PTX 50 and 100 $mg\,kg^{-1}$ were below detection limits and less than 0.1 $\mu g\,g^{-1}$, respectively.

In vitro cytotoxicity

NK105 was tested on 12 human tumour cell lines derived from lung, gastric, oesophagus, colon, breast, and ovarian tumours. Similar dose–response curves were noted for PTX and NK105 (data not shown). Furthermore, the IC_{50} values of NK105 were similar to those of PTX at 48 and 72 h, indicating that both NK105 and PTX showed equivalent cytotoxic activity *in vitro* (Table 2).

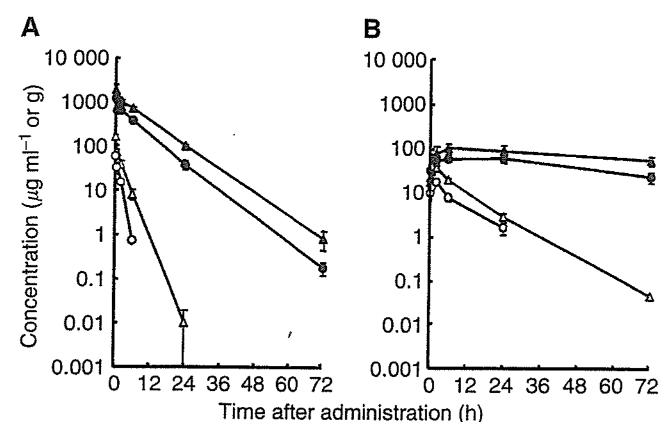

Figure 2 Plasma and tumour concentrations of PTX after single i.v. administration of NK105 or PTX to Colon 26-bearing CDF1 mice. Plasma (**A**) and tumour (**B**) concentrations of PTX after NK105 administration at a PTX-equivalent dose of 50 $mg\,kg^{-1}$ (●), NK105 at a PTX-equivalent dose of 100 $mg\,kg^{-1}$ (▲), PTX 50 $mg\,kg^{-1}$ (○) and PTX 100 $mg\,kg^{-1}$ (△).

In vivo antitumour activity

BALB/c mice bearing s.c. HT-29 colon cancer tumours showed decreased tumour growth rates after the administration of PTX and NK105. However, NK105 exhibited superior antitumour activity as compared with PTX ($P<0.001$). The antitumour activity of NK105 administered at a PTX-equivalent dose of 25 $mg\,kg^{-1}$ was comparable to that obtained after the administration of free PTX 100 $mg\,kg^{-1}$. Tumour suppression by NK105 increased in a dose-dependent manner. Tumours disappeared after the first dosing to mice treated with NK105 at a PTX-equivalent dose of 100 $mg\,kg^{-1}$, and all mice remained tumour-free thereafter (Figure 3A). In addition, less weight loss was induced in mice, which were given NK105 100 $mg\,kg^{-1}$ than in those that were given the same dose of free PTX (Figure 3B).

Table 2 IC_{50} values (μM) of PTX and NK105 in various cell lines

		48 h		72 h	
Cancer	**Cell line**	**NK105**	**PTX**	**NK105**	**PTX**
Oesophageal cancer	TE-1	>1.0	>1.0	0.01	0.02
	TE-8	0.02	0.02	0.01	0.01
Lung cancer	PC-14	0.01	0.01	0.01	0.01
	PC-14/TXT	0.15	0.09	0.08	0.06
	H460	ND	ND	0.03	0.01
Breast cancer	MCF-7	>1.0	>1.0	0.01	0.01
Stomach cancer	MKN-28	0.03	0.03	0.01	0.21
	MKN-45	0.02	0.07	0.01	0.02
Colon cancer	DLD-1	0.95	0.26	0.29	0.20
	HT-29	0.01	0.01	0.01	0.01
	HCT116	ND	ND	0.03	0.01
Ovarian cancer	MCAS	0.01	0.01	0.01	0.01
	OVCAR-3	>1.0	>1.0	>1.0	>1.0
Pancreatic cancer	AsPC-1	ND	ND	0.02	0.02
	PAN-9	ND	ND	0.03	0.02
	PAN-3	ND	ND	0.010	0.004

PTX = paclitaxel; ND = not done.

Table 1 Pharmacokinetic parameters for the plasma and tumour concentrations of paclitaxel after single i.v. administration of NK105 and PTX to Colon 26-bearing CDF1 mice

Treatment	**Dose ($mg\,kg^{-1}$)**	**$C_{5\,min}$ ($\mu g\,ml^{-1}$)**	**$t_{1/2}z$ (h)**	**AUC_{0-t} ($\mu g\,h\,ml^{-1}$)**	**$AUC_{0-inf.}$ ($\mu g\,h\,ml^{-1}$)**	**CL_{tot} ($ml\,h\,kg^{-1}$)**	**V_{ss} ($ml\,kg^{-1}$)**
Plasma							
PTX	50	59.32	0.98	90.2[a]	91.3	547.6	684.6
PTX	100	157.67	1.84	309.0[b]	309.0	323.6	812.2
NK105	50	1157.03	5.99	7860.9[c]	7862.3	6.4	46.4
NK105	100	1812.37	6.82	15 565.7[c]	15 573.6	6.4	54.8
		C_{max} ($\mu g\,ml^{-1}$)	**T_{max} (h)**	**$t_{1/2}z$ (h)**	**AUC_{0-t} ($\mu g\,h\,ml^{-1}$)**	**$AUC_{0-inf.}$ ($\mu g\,h\,ml^{-1}$)**	
Tumour							
PTX	50	12.50	2.0	7.02	120.8[b]	133.0	
PTX	100	28.57	0.5	8.06	330.4[c]	331.0	
NK105	50	42.45	24.0	35.07	2360.1[c]	3192.0	
NK105	100	71.09	6.0	73.66	3884.9[c]	7964.5	

i.v. = intravenous; $C_{5\,min}$ = plasma concentration at 5 min; $t_{1/2}z$ = half-life at the terminal phase; AUC = area under the curve; CL_{tot} = total body clearance; V_{ss} = volume of distribution at steady state; T_{max} = time of maximum concentration; PTX = paclitaxel. Parameters were calculated from the mean value of three or two mice by noncompartmental analysis. [a]AUC_{0-6h}. [b]AUC_{0-24h}. [c]AUC_{0-72h}.

© 2005 Cancer Research UK

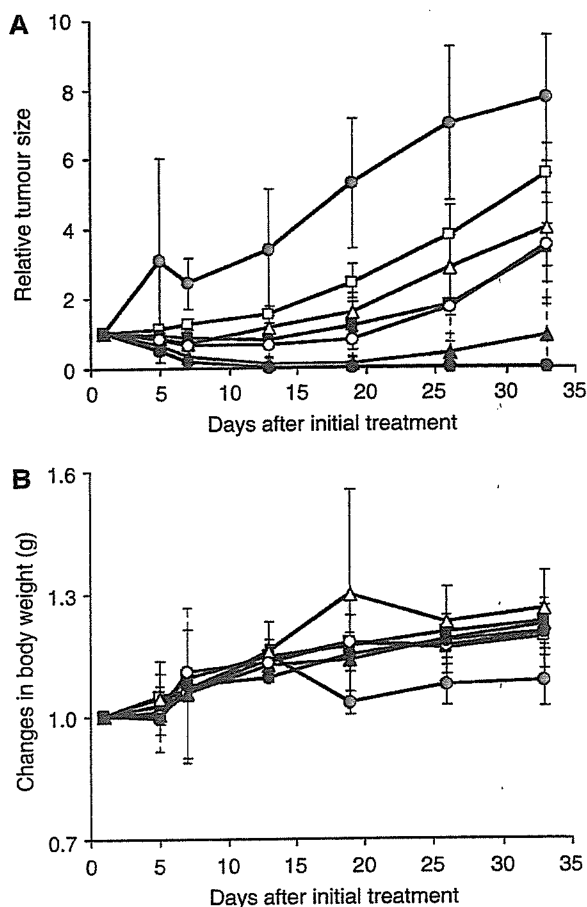

Figure 3 Relative changes in HT-29 tumour growth rates in nude mice. (**A**) Effects of PTX (open symbols) and NK105 (closed symbols). PTX and NK105 were injected i.v. once weekly for 3 weeks at PTX-equivalent doses of 25 mg kg^{-1} (□, ■), 50 mg kg^{-1} (△, ▲), and 100 mg kg^{-1} (○, ●), respectively. Saline was injected to control animals (●). (**B**) Changes in relative body weight. Data were derived from the same mice as those used for the present study.

Neurotoxicity of PTX and NK105

Treatment with PTX has resulted in cumulative sensory-dominant peripheral neurotoxicity in humans, characterised clinically by numbness and/or paraesthesia of the extremities. Pathologically, axonal swelling, vesicular degeneration, and demyelination were observed. We, therefore, examined the effects of free PTX and NK105 using both electrophysiological and morphological methods.

Prior to drug administration, there were no significant differences in the amplitude of caudal sensory nerve action potential (caudal SNAP) between two drug administration groups. On day 6 after the last dosing (at week 6), the amplitude of the caudal SNAP in the control group increased in association with rat maturation. The amplitude was significantly smaller in the PTX group than in the control group ($P<0.01$), while the amplitude was significantly larger in the NK105 group than in the PTX group ($P<0.05$) and was comparable between the NK105 group and the control group (Figure 4A). Histopathological examination of longitudinal paraffin-embedded sections of the sciatic nerve 5 days after the sixth weekly injection revealed degenerative changes. The NK105 administration group showed only a few degenerative myelinated fibres in contrast to the PTX administration group, which indicated markedly more numerous degenerative myelinated fibres ($P<0.001$) (Figure 4B and C) and Table 3.

DISCUSSION

A pharmacokinetic study revealed that the plasma AUC of NK105 was approximately 90-fold higher than that of free PTX in the present rodent models. Prolonged circulation of NK105 in the blood due to the EPR effect was associated with a significant increase in the tumour AUC. In fact, the tumour AUC of NK105 was approximately 25-fold higher than that of free PTX (Figure 2B). In mice, accordingly, NK105 exhibited stronger antitumour activity than free PTX (Figure 3A). However, it is still debatable whether or not the enhanced accumulation of an anticancer drug into a tumour is sufficient in leading the drug to exert its antitumour activity *in vivo*.

Jain *et al* have reported that the convective passage of large drug molecules into the core of solid tumours could be impeded by abnormally high interstitial pressures in solid tumours. However, they also admitted that low-molecular-weight anticancer agents might be harmful to normal organs because they can leak out of normal blood vessels freely; they finally concluded that one useful strategy for evading the barriers to drug dispersion would be to inject patients with drug carriers, such as liposomes, filled with low-molecular-weight drugs (Jain, 1994). In this case, liposomes should have sufficient time to exit from the site of tumour blood vessel leakage and to accumulate at reasonably high dose levels in the surrounding interstitium. Subsequently, low-molecular-weight drugs packed within liposomes should be released gradually so that they can be dispersed throughout the tumour. However, Unezaki *et al* have used fluorescence-labelled PEG-liposomes and described that the area of highest fluorescence was located outside tumour vessels, almost all around the vessel wall, even 2 days after drug injection (Unezaki *et al*, 1996). Therefore, the study suggested that although PEG-liposomes can be delivered effectively to a solid tumour via the EPR effect, the formulation would not be distributed sufficiently to cancer cells distant from tumour vessels because liposomes are too large to scamper about in the tumour interstitium. Liposomes have been suggested to be too stable to allow the drug therein to be released easily. Therefore, PEG-liposomes have been speculated to be not so effective against cancers in which the tumour vessel network is irregular and loose because of an abundant collagen-rich matrix. Such cancers include scirrhous cancer of the stomach and pancreatic cancer. In fact, Doxil®, a PEG-liposomal DXR, is known to be effective clinically against ovarian cancer and breast cancer, both of which are characterised by a high density of tumour microvessels; however, the drug is not effective against stomach cancer and pancreatic cancer (Muggia, 2001).

There are several possible reasons why NK105 exhibited higher antitumour activity in the present study as compared with free PTX: (1) since NK105 is very stable in the circulation and exhibits a markedly higher plasma AUC than free PTX, it accumulates better in tumour tissue than does free PTX due to the EPR effect; (2) NK105 is relatively small in size (85 nm) as compared with Doxil (100 nm), thus explaining its more uniform distribution in tumour tissue and its greater accumulation in cancer cells throughout cancer tissue. Savic *et al* (2003) have recently reported that polymeric micelles could internalise into cells to localise in several cytoplasmic organelles; and (3) a polymeric micelle carrier system for a drug has the potential to allow the effective sustained release of the drug inside a tumour following the accumulation of micelles into tumour tissue. Regarding NK105 in particular, this sustained release begins at a PTX-equivalent dose of $<1\,\mu g\,ml^{-1}$ (data not shown). Consequently, released PTX becomes distributed throughout tumour tissue and internalises into cancer cells to kill them.

© 2005 Cancer Research UK

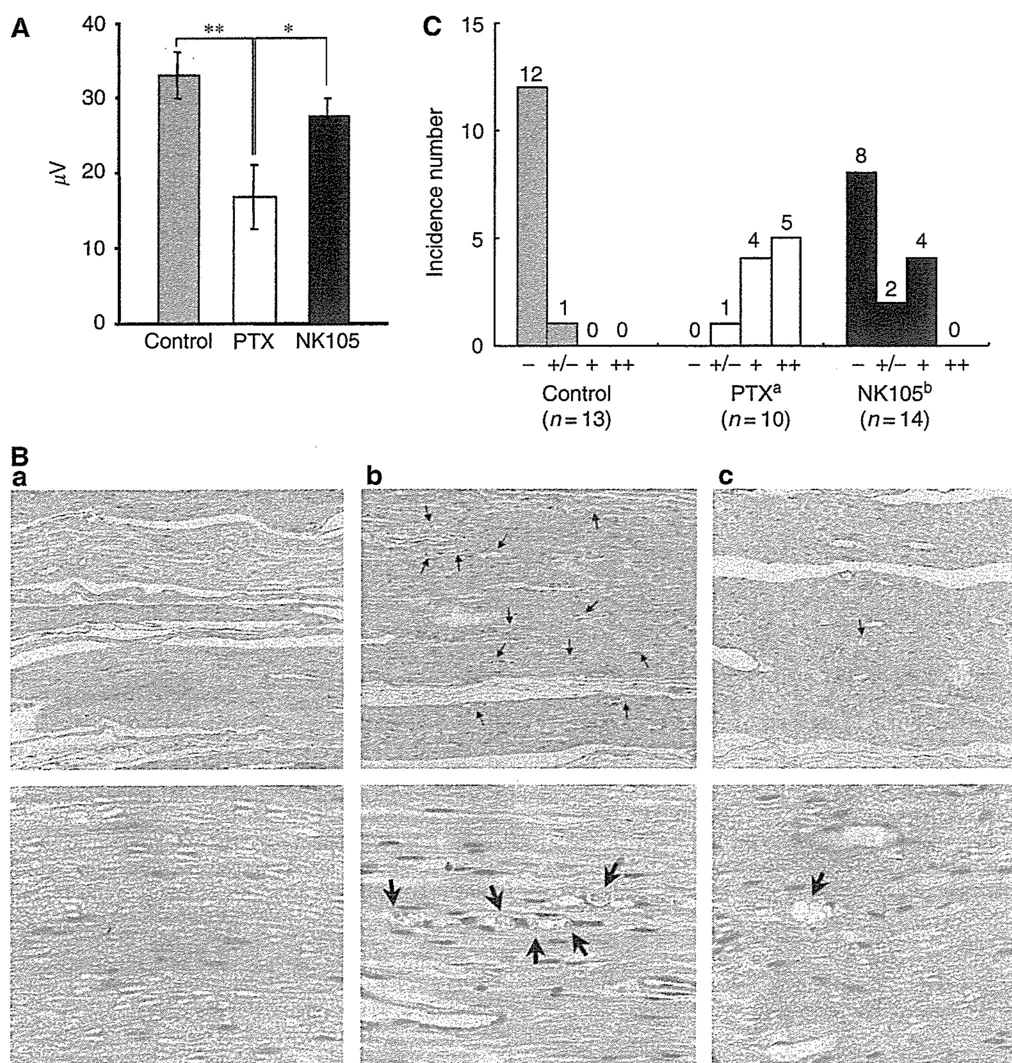

Figure 4 Incorporation of PTX into polymeric micelles diminishes neurotoxicity. (**A**) Effects of PTX or NK105 on the amplitude of rat caudal sensory nerve action potentials as examined 5 days after weekly injections for 6 weeks. Rats ($n = 14$) were injected with NK105 (■) or PTX (□) at a PTX-equivalent dose of 7.5 mg kg^{-1}. Glucose (5%) was also injected in the same manner to animals in the control group (■). *$P<0.05$, **$P<0.01$. (**B**) Histopathological changes in the sciatic nerve of rats. Degenerating myelinated nerve fibres (arrow) were examined in the longitudinal section of the sciatic nerve (H & E) 5 days after weekly injections for 6 weeks with 5% glucose (a), PTX (b), and NK105 (c) at a PTX-equivalent dose of 7.5 mg kg^{-1}. Magnification, ×100 (upper) and ×400 (lower). (**C**) Incidences of degenerating myelinated nerve fibres in rats treated with PTX or NK105. NK105 or PTX was administered i.v. at a weekly dose of 7.5 mg kg^{-1} for 6 consecutive weeks to female rats. The degenerating myelinated fibre score was defined as follows: −, no degenerative changes; +/−, very slight degree of the degenerative changes (scattered, single fibres affected); +, slight degree of degenerative changes (scattered small groups of degenerative myelinated fibres); + +, moderate degree of degenerative changes (disseminated degenerative myelinated fibres); + + +, marked degree of degenerative changes (confluent groups of affected fibres). [a]$P<0.001$ vs vehicle-treated animals. [b]$P<0.001$ vs PTX-treated animals.

To date, PTX preparations that are categorised to DDSs have been developed. Among them, clinical trials are currently ongoing for the following drugs: CT-2103, polyglutamate-conjugated PTX (Singer *et al*, 2003); ABI-007, PTX coated with albumin (Ibrahim *et al*, 2002); and Genexol-PM, PTX micelle in which PTX is simply solubilised (Kim *et al*, 2004). The advantage commonly shared with these dosage forms is that they are injectable i.v. without the mixture of Cremophor EL and ethanol, which potentially provoke serious allergic reactions. The block copolymer used for forming NK105 micellar nanoparticles is nonimmunogenic and is injectable i.v. without Cremorphor EL and ethanol. Therefore, this dosage form is expected to possess a clinical advantage, which is similar to that of the above PTX dosage forms. Now, what is the difference between NK105 and other PTX dosage forms? ABI-007 and Genexol-PM were found to have the AUC and tumour AUC, which are nearly comparable or rather slightly lower than those of free PTX. Furthermore, the plasma AUC and tumour AUC are 11.5- and 11.8-fold higher, respectively, for CT-2103 than for free PTX, but they are markedly low as compared with those of NK105. Respective studies have employed proper tumours and proper rodent models. However, NK105 was forecasted to have markedly high plasma and tumour AUC as compared with those of other PTX dosage forms.

Regarding the toxicity profiles, the repeated administration of NK105 to rats at 7-day intervals produced less toxic effects on peripheral nerves than free PTX. This reduced the neurotoxicity of

© 2005 Cancer Research UK

Table 3 Incidence of degenerating myelinated fibres in rats treated with PTX or NK105

Treatment	n[a]	Degenerating myelinated nerve fibre score[b]				
		–	+/–	+	++	+++
Control (vehicle)	13	12	1			
PTX[c]	10		1	4	5	
NK105[d]	14	8	2	4		

PTX = paclitaxel. Vehicle, NK105 or PTX was administered i.v. at a weekly dose of 7.5 mg kg^{-1} for 6 consecutive weeks to female rats. [a]Total number of animals accounted for that experimental condition. [b]Degenerating myelinated fibre score was defined as follows: –, no degenerative changes; +/–, very slight degree of the degenerative changes (scattered, single fibres affected); +, slight degree of degenerative changes (scattered small groups of degenerative myelinated fibers); ++, moderate degree of degenerative changes (disseminated degenerative myelinated fibers); +++, marked degree of degenerative changes (confluent groups of affected fibres). [c]$P<0.001$ vs vehicle-treated animals. [d]$P<0.001$ vs PTX-treated animals.

NK105, which was demonstrated for the first time by both histopathological and physiological methods and was probably attributable to the less distribution of PTX into normal neural tissue following NK105 administration, since the volume of distribution at steady state (V_{ss}) of NK105 was 100-fold lower than that of free PTX. Regarding bone marrow toxicity, there was no difference between PTX and NK105 when 37.5 mg kg^{-1} of PTX-equivalent dose was administered to rats weekly for 4 consecutive weeks (data not shown). These data indicate that NK105 warrants a clinical evaluation.

ACKNOWLEDGEMENTS

We thank Dr H Uchino, Miss M Araake, and Mrs H Koike for their technical assistance. We are also grateful to Mrs K Shiina and Miss H Orita for their secretarial assistance. This work was supported by a Grant-in-Aid from the Ministry of Health, Labor and Welfare of Japan (Y Matsumura).

REFERENCES

Carney DN (1996) Chemotherapy in the management of patients with inoperable non-small cell lung cancer. *Semin Oncol* **23:** 71–75

Hamaguchi T, Matsumura Y, Shirao Y, Shimada Y, Yamada Y, Muro Y, Okusaka T, Ueno H, Ikeda M, Watanabe N (2003) Phase I study of novel drug delivery system, NK911, a polymer micelle encapsulated doxorubicin. *Proc Am Soc Clin Oncol* **22:** 571

Ibrahim NK, Desai N, Legha S, Soon-Shiong P, Theriault RL, Rivera E, Esmaeli B, Ring SE, Bedikian A, Hortobagyi GN, Ellerhorst JA (2002) Phase I and pharmacokinetic study of ABI-007, a Cremophor-free, protein-stabilized, nanoparticle formulation of paclitaxel. *Clin Cancer Res* **8:** 1038–1044

Jain RK (1994) Barriers to drug delivery in solid tumours. *Sci Am* **271:** 58–65

Kataoka K, Kwon GS, Yokoyama M, Okano T, Sakurai Y (1993) Block copolymer micelles as vehicles for drug delivery. *J Control Rel* **24:** 119–132

Khayat D, Antoine EC, Coeffic D (2000) Taxol in the management of cancers of the breast and the ovary. *Cancer Invest* **18:** 242–260

Kim TY, Kim DW, Chung JY, Shin SG, Kim SC, Heo DS, Kim NK, Bang YJ (2004) Phase I and pharmacokinetic study of Genexol-PM, a cremophor-free, polymeric micelle-formulated paclitaxel, in patients with advanced malignancies. *Clin Cancer Res* **10:** 3708–3716

Kwon GS, Suwa S, Yokoyama M, Okano T, Sakurai Y (1994) Enhanced tumour accumulation and prolonged circulation times of micelle-forming poly(ethylene oxide-aspartic) block copolymer-adriamycin conjugate. *J Control Rel* **29:** 17–23

Maeda H, Wu J, Sawa T, Matsumura Y, Hori K (2000) Tumour vascular permeability and the EPR effect in macromolecular therapeutics: a review. *J Control Rel* **65:** 271–284

Matsumura Y, Maeda H (1986) A new concept for macromolecular therapeutics in cancer chemotherapy: mechanism of tumouritropic accumulation of proteins and the antitumour agent smancs. *Cancer Res* **46:** 6387–6392

Muggia FM (2001) Liposomal encapsulated anthracyclines: new therapeutic horizons. *Curr Oncol Rep* **3:** 156–162

Nakanishi T, Fukushima S, Okamoto K, Suzuki M, Matsumura Y, Yokoyama M, Okano T, Sakurai Y, Kataoka K (2001) Development of the polymer micelle carrier system for doxorubicin. *J Control Rel* **74:** 295–302

Rowinsky EK, Chaudhry V, Forastiere AA, Sartorius SE, Ettinger DS, Grochow LB, Lubejko BG, Cornblath DR, Donehower RC (1993) Phase I and pharmacologic study of paclitaxel and cisplatin with granulocyte colony-stimulating factor: neuromuscular toxicity is dose-limiting. *J Clin Oncol* **11:** 2010–2020

Rowinsky EK, Donehower RC (1995) Paclitaxel (taxol). *N Engl J Med* **332:** 1004–1014

Savic R, Luo L, Eisenberg A, Maysinger D (2003) Micellar nanocontainers distribute to defined cytoplasmic organelles. *Science* **300:** 615–618

Singer JW, Baker B, De Vries P, Kumar A, Shaffer S, Vawter E, Bolton M, Garzone P (2003) Poly-(L)-glutamic acid-paclitaxel (CT-2103) [XYOTAX], a biodegradable polymeric drug conjugate: characterization, preclinical pharmacology, and preliminary clinical data. *Adv Exp Med Biol* **519:** 81–99

Unezaki S, Maruyama K, Hosoda J, Nagai I, Koyanagi Y, Nakata M, Ishida O, Iwatsuru M, Tsuchiya S (1996) Direct measurement of the extravasation of polyethylene glycol-coated liposomes into solid tumour tissue by *in vivo* fluorescence microscopy. *Int J Pharmacol* **144:** 11–17

Wasserheit C, Frazein A, Oratz R, Sorich J, Downey A, Hochster H, Chachoua A, Wernz J, Zeleniuch-Jacquotte A, Blum R, Speyer J (1996) Phase II trial of paclitaxel and cisplatin in women with advanced breast cancer: an active regimen with limiting neurotoxicity. *J Clin Oncol* **14:** 1993–1999

Weiss RB, Donehower RC, Wiernik PH, Ohnuma T, Gralla RJ, Trump DL, Baker Jr JR, Van Echo DA, Von Hoff DD, Leyland-Jones B (1990) Hypersensitivity reactions from taxol. *J Clin Oncol* **8:** 1263–1268

Yokoyama M, Miyauchi M, Yamada N, Okano T, Sakurai Y, Kataoka K, Inoue S (1990) Polymer micelles as novel drug carrier:adriamycin-conjugated poly(ethylene glycol)-poly(aspartic acid) block copolymer. *J Control Rel* **11:** 269–278

Yokoyama M, Okano T, Sakurai Y, Ekimoto H, Shibazaki C, Kataoka K (1991) Toxicity and antitumour activity against solid tumours of micelle-forming polymeric anticancer drug and its extremely long circulation in blood. *Cancer Res* **51:** 3229–3236

Yokoyama M, Okano T, Sakurai Y, Fukushima S, Okamoto K, Kataoka K (1999) Selective delivery of adriamycin to a solid tumour using a polymeric micelle carrier system. *J Drug Target* **7:** 171–186

© 2005 Cancer Research UK

0022-5347/05/1735-1767/0
THE JOURNAL OF UROLOGY®
Copyright © 2005 by AMERICAN UROLOGICAL ASSOCIATION
Vol. 173, 1767–1771, May 2005
Printed in U.S.A.
DOI: 10.1097/01.ju.0000154632.11824.4d

DNA HYPERMETHYLATION ON MULTIPLE CpG ISLANDS ASSOCIATED WITH INCREASED DNA METHYLTRANSFERASE DNMT1 PROTEIN EXPRESSION DURING MULTISTAGE UROTHELIAL CARCINOGENESIS

TOHRU NAKAGAWA, YAE KANAI,* SAORI USHIJIMA, TADAICHI KITAMURA, TADAO KAKIZOE AND SETSUO HIROHASHI

From the Pathology Division, National Cancer Center Research Institute (TN, YK, SU, SH), Department of Urology, Faculty of Medicine, Tokyo University (TN, TKi) and National Cancer Center (TKa), Tokyo Japan

ABSTRACT

Purpose: We elucidated the significance of aberrant DNA methylation on multiple CpG islands and its correlation with DNA methyltransferase DNMT1 protein expression during urothelial carcinogenesis.

Materials and Methods: We examined the DNA methylation status on multiple CpG islands by methylation specific polymerase chain reaction and combined bisulfite restriction enzyme analysis in 12 specimens of normal urothelium, 23 of noncancerous urothelium showing no remarkable histological changes obtained from patients with bladder cancer (NBC) and 70 of transitional cell carcinoma (TCC).

Results: DNA methylation on CpG islands of the *p16* (0%, 17% and 21%) and *death-associated protein kinase* (13%, 33% and 29%) genes, and methylated in tumor-2 (56%, 60% and 76%), 12 (0%, 6% and 30%), 25 (25%, 27% and 35%) and 31 (45%, 56% and 79%) clones was detected in normal urothelium, NBCs and TCCs, respectively. The incidence of concurrent DNA hypermethylation on 3 or more CpG islands in NBCs (38%) was significantly higher than that in normal urothelium (0%, $p = 0.0455$) and even higher in TCCs (59%, $p = 0.0043$). The incidence of the CpG island methylator phenotype in nonpapillary carcinomas (nodular invasive carcinomas and their precursors, ie flat carcinoma in situ, 71%) was significantly higher than in papillary carcinomas (40%, $p = 0.0143$). In all specimens examined concurrent DNA hypermethylation on 3 or more CpG islands significantly correlated with immunohistochemically evaluated DNMT1 protein over expression ($p = 0.0167$).

Conclusions: DNA hypermethylation on multiple CpG islands in association with DNMT1 protein over expression may participate in multistage urothelial carcinogenesis even at the precancerous stage and particularly in the development of nodular invasive carcinomas of the bladder.

KEY WORDS: carcinoma, transitional cell; bladder; CpG islands; phenotype; DNA

DNA methylation has important roles in transcriptional regulation, chromatin remodeling and genomic stability. Overall DNA hypomethylation accompanied by region specific hypermethylation is generally observed in human cancers.[1] Aberrant DNA methylation may have roles in carcinogenesis as a result of 1) increased gene mutagenicity due to the deamination of 5-methylcytosine to thymine, 2) the possible association of aberrant DNA methylation with allelic loss and 3) the repression of gene transcription through the methylation of CpG islands in regulatory regions of specific genes, including tumor suppressor genes.[1] In transitional cell carcinomas (TCCs) of the bladder hypermethylation on CpG islands around the promoter region and decreased expression of tumor suppressor genes, such as the *p16* and *E-cadherin* genes, have been reported.[2,3] Regional DNA hypermethylation correlates significantly with poor prognosis in patients with TCC.[2] However, only a limited number of groups have examined aberrant DNA methylation with regard to precancerous conditions and the histological heterogeneity of TCCs.

Increased mRNA and protein expression of DNA methyltransferase DNMT1 is reported to correlate significantly with the CpG island methylator phenotype (CIMP), defined as frequent DNA hypermethylation on CpG islands that are not normally methylated,[4] in colorectal and stomach cancers.[5,6] We have previously reported that DNMT1 protein expression is already increased in noncancerous urothelium showing no remarkable histological changes obtained from patients with bladder cancer (NBC), preceding the increase in cell proliferative activity reflected by the proliferating cell nuclear antigen (PCNA) labeling index.[7] Such urothelium can be considered precancerous because it may be exposed to carcinogens in the urine. Progressively increasing expression of DNMT1 protein is particularly associated with the development of flat carcinoma in situ (CIS), which is considered to be a precursor of nodular invasive carcinoma of the bladder.[7] However, to our knowledge no studies have determined whether in fact DNMT1 over expression results in DNA hypermethylation on CpG islands during urothelial carcinogenesis.

To determine the significance of aberrant DNA methylation and examine whether increased DNMT1 protein expression is the underlying mechanism for this aberrant

Submitted for publication August 5, 2004.
Supported by a Grant-in-Aid for the Second Term Comprehensive 10-Year Strategy for Cancer Control and a Grant-in-Aid for Cancer Research, Ministry of Health, Labor and Welfare of Japan, and a Research Resident Fellowship from the Foundation for Promotion of Cancer Research in Japan (TN).
* Correspondence: Pathology Division, National Cancer Center Research Institute, 5-1-1 Tsukiji, Chuo-ku, Tokyo 104-0045, Japan (FAX: 81-3-3248-2463; e-mail: ykanai@ncc.go.jp).

methylation during human urothelial carcinogenesis we examined DNA methylation status on multiple CpG islands in normal urothelium, NBCs and TCCs. We also examined the correlation between DNA methylation status and immunohistochemically evaluated DNMT1 protein expression.

MATERIALS AND METHODS

Patients and tissue samples. A total of 23 specimens of NBC and 70 of TCC were obtained from surgically resected specimens of patients who underwent radical cystectomy (40) or transurethral resection of bladder tumor (15) at National Cancer Center Hospital, Tokyo, Japan. The study group comprised 44 men and 11 women with a mean age ± SD of 62.4 ± 11.9 years (range 39 to 89). The 70 TCC specimens were classified histologically as pTa in 29, pTis in 14, pT1 in 7 and pT2 to pT3 in 20 according to criteria proposed by the International Union Against Cancer.[8] That is, there were 29 papillary (noninvasive, pTa) tumors and 41 nonpapillary tumors (flat CIS or pTis and invasive carcinoma, pT1 to pT3). For comparison, 12 specimens of normal urothelium were also obtained from specimens surgically resected from 12 patients who underwent total pelvic exenteration for primary or locally recurrent rectal cancers. This patient group comprised 9 men and 3 women with a mean age of 56.1 ± 9.0 years (range 37 to 70). For 89 of these 105 specimens we have previously reported the results of immunohistochemical examination for DNMT1.[7]

Methylation specific polymerase chain reaction (PCR) (MSP) and combined bisulfite restriction enzyme analysis (COBRA). Sections (10 μm) from formalin fixed, paraffin embedded specimens were mounted on microscope slides, deparaffinized and stained with hematoxylin and eosin. Cancerous and noncancerous urothelium was collected under a stereoscopic microscope using a fine needle, avoiding potential contamination between each cell type or with stromal and inflammatory cells (fig. 1). DNA was isolated from microdissected specimens by a standard procedure involving proteinase-K treatment, phenol-chloroform extraction and ethanol precipitation.

Bisulfite conversion of DNA was done with a CpGenome DNA Modification Kit (Intergen, Purchase, New York) in accordance with manufacturer instructions. DNA methylation status on CpG islands of the *p16* gene was determined by MSP[9] using primer sets provided in a CpG WIZ amplification kit (Intergen). DNA methylation status on the *death-associated protein kinase* (*DAPK*) gene, and on methylated in tumor (MINT)-2, 12, 25 and 31 clones was determined by COBRA.[10] Bisulfite modified DNA was amplified by PCR using previously described primers[4,11] and digested with restriction enzymes, including BstUI for the *DAPK* gene, and MINT-2 and 31 clones, MaeII for the MINT-12 clone and RsaI for the MINT-25 clone. Reaction products were separated electrophoretically on 3% agarose gel and stained with ethidium bromide. Signal intensity was measured with an image analyzer (Model FMBIO-2, Takara, Ohtsu, Japan).

Statistics. Correlations between the incidence of concurrent DNA hypermethylation on 3 or more CpG islands or CIMP on 1 hand, and clinicopathological parameters or DNMT1 immunoreactivity on the other hand were analyzed by the chi-square test with $p < 0.05$ considered significant.

RESULTS

DNA methylation status on multiple CpG islands in noncancerous urothelium and TCCs. Figure 2 shows examples of PCR products from MSP and COBRA. DNA methylation on CpG islands of the *p16* gene was detected in 0 of the 9 examined normal urothelium samples (0%), in 3 of the 18 examined NBCs (17%) and in 13 of the 62 examined TCCs (21%). DNA methylation of the *DAPK* gene was detected in 1 of the 8 normal urothelium samples (13%), in 6 of the 18 NBCs (33%) and in 18 of the 63 TCCs (29%). DNA methylation of the MINT-2 clone was detected in 5 of the 9 normal urothelium samples (56%), in 13 of the 22 NBCs (60%) and in 52 of the 68 TCCs (76%). DNA methylation of the MINT-12 clone was detected in 0 of the 8 normal urothelium samples (0%), in 1 of the 18 NBCs (6%) and in 20 of the 67 TCCs (30%). DNA methylation of the MINT-25 clone was detected in 2 of the 8 normal urothelium samples (25%), in 4 of the 15 NBCs (27%) and in 22 of the 62 TCCs (35%). DNA methylation of the MINT-31 clone was detected in 5 of the 11 normal urothelium samples (45%), in 10 of the 18 NBCs (56%) and in 52 of the 66 TCCs (79%). Although DNA methylation on some CpG islands was detected even in normal urothelium, the incidence in normal urothelium did not correlate with patient age (data not shown). Generally the incidence of DNA methylation on each CpG island increased progressively from normal urothelium to NBCs and then to TCCs.

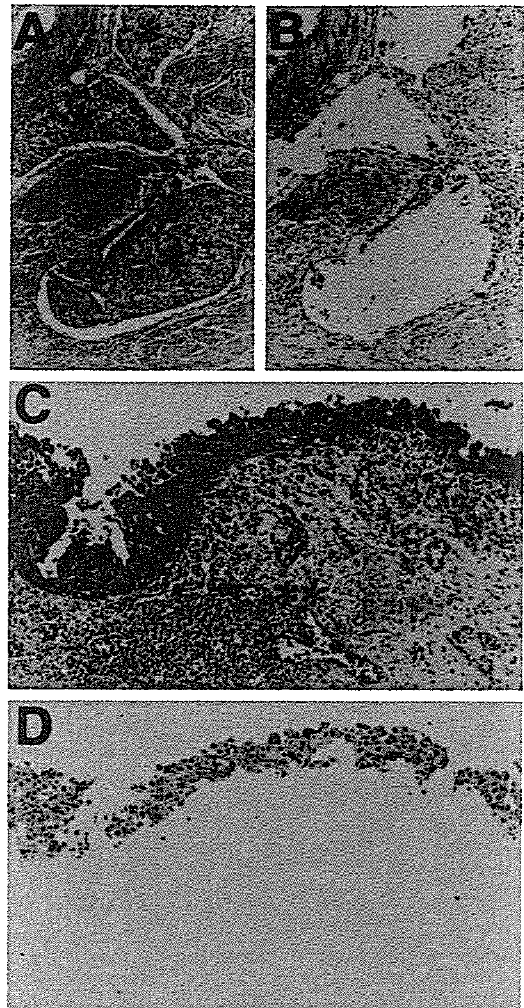

FIG. 1. Representative specimens of TCC, including specimen T18 of nodular invasive carcinoma (*A* and *B*) and specimen T31 of CIS (*C* and *D*) before (*A* and *C*), during (*D*) and after (*B*) microdissection. Single asterisks indicate invasive carcinoma specimen (*A*) collected without contamination with stromal and inflammatory cells (*B*). Double asterisks indicate subepithelial tissue (*C*) removed to avoid contamination (*D*) before collecting flat CIS specimens. Reduced from ×50 (*A* and *B*) and ×90 (*C* and *D*)

Previously described criteria have defined cancers showing DNA hypermethylation on 3 or more CpG islands that are not methylated in an age dependent manner as CIMP positive when 5 or more of such CpG islands are examined.[4] Figure 3 shows DNA methylation status on each CpG island in 87 specimens of normal urothelium, NBC and TCC, in

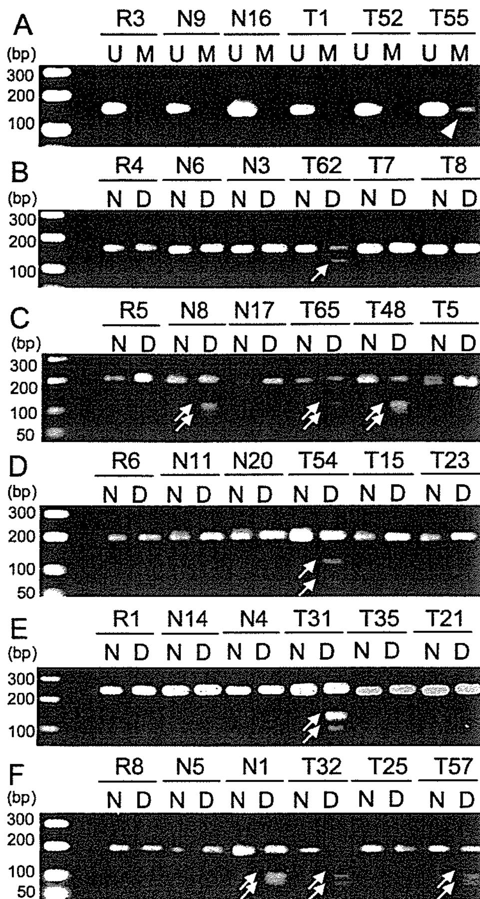

FIG. 2. Examples of PCR products from DNA methylation analyses of multiple CpG islands in patients with or without bladder cancer. DNA methylation status on CpG islands of *p16* gene (*A*) was evaluated by MSP. In this analysis PCR products generated by primer sets reflected presence of methylated (*M*, arrowhead) and unmethylated (*U*) genes. DNA methylation on CpG islands of *DAPK* (*B*) gene, and MINT-2, 12, 25 and 31 clones (*C* to *F*, respectively) was evaluated by COBRA. In this analysis only methylated genes (arrows) were digested by restriction enzymes. *R*, normal urothelium obtained from patients who underwent total pelvic exenteration for rectal cancer. *N*, noncancerous urothelium showing no remarkable histological changes obtained from patients with bladder cancer. *T*, TCC. *N*, non-digestion with restriction enzyme. *D*, digestion with restriction enzyme.

which 5 or all 6 CpG islands could be evaluated. However, we examined DNA methylation status on only 4 or fewer CpG islands in the remaining 18 specimens because of a shortage of DNA extracted from the microdissected samples. Concurrent DNA methylation on 3 or more CpG islands was detected in 0 of the 8 normal urothelium samples (0%), 6 of the 16 NBCs (38%) and 37 of the 63 TCCs (59%). Such TCCs were considered CIMP positive based on described criteria.[4] The incidence of concurrent DNA hypermethylation on 3 or more CpG islands increased progressively from normal urothelium to NBCs and then to TCCs (chi-square test p = 0.0043). Even in NBCs it was significantly higher than in normal urothelium (chi-square test p = 0.0455).

Correlation between DNA methylation status on multiple CpG islands and clinicopathological parameters in TCC 23 (52%). Of the 44 specimens of superficial carcinoma (pTa, pTis and pT1) and 14 (74%) of 19 of invasive carcinoma (pT2 to pT4) were CIMP positive. Invasion depth (pTa, pTis and pT1 vs pT2 to pT4) did not significantly correlate with CIMP (chi-square test p = 0.1131). Ten of 25 specimens (40%) of papillary carcinoma (pTa) and 27 of 38 (71%) of nonpapillary carcinoma (flat CIS or pTis and invasive carcinoma pT1 or greater) were CIMP positive. The incidence of CIMP was

Specimen	Number of methylated CpG islands	Sample name	pT	DNMT1 protein expression	p16	DAPK	MINT-2	MINT-12	MINT-25	MINT-31
Normal urothelia obtained from patients with rectal cancer	<3	R1		−						
		R2		−						
		R3		−		NE				
		R4		−						
		R5		+						
		R6		+						
		R7		−						
		R8		−						
Non-cancerous urothelia showing no remarkable histological changes obtained from patients with bladder cancer	<3	N1		−						
		N2		−					NE	
		N3		+						
		N4		+		NE				
		N5		−		NE				
		N6		+						
		N7		−						
		N8		−						
		N9		+					NE	
		N10		−						
	≥3	N11		−						
		N12		−						
		N13		+						
		N14		+						
		N15		−						
		N16		+						
Transitional cell carcinomas	<3 (CIMP-negative)	T1	pTa	−						
		T2	pTa	−					NE	
		T3	pTa	−						
		T4	pTa	−						
		T5	pTa	−						
		T6	pT2−3	++				NE		
		T7	pTa	++						
		T8	pTis	++						
		T9	pTis	++					NE	
		T10	pTa	+						NE
		T11	pT2−3	+						
		T12	pTis	++						
		T13	pTa	−				NE		
		T14	pTa	−						
		T15	pTa	−						
		T16	pTa	−						
		T17	pT1	+						
		T18	pT2−3	+						
		T19	pT2−3	+						
		T20	pTis	++						
		T21	pTis	++						
		T22	pTa	−	NE					
		T23	pTa	−						
		T24	pTa	−						
		T25	pT2−3	−						
		T26	pTa	−						
	≥3 (CIMP-positive)	T27	pTa	−						
		T28	pT2−3	+						
		T29	pT2−3	+		NE				
		T30	pT1	++						
		T31	pTis	++						
		T32	pT2−3	NE	NE					
		T33	pTa	+	NE					
		T34	pT2−3	−						
		T35	pTa	−						
		T36	pT2−3	+						
		T37	pTa	+						
		T38	pTis	+		NE				
		T39	pT1	++		NE				
		T40	pT2−3	−						
		T41	pT1	+						
		T42	pTis	++						
		T43	pT2−3	++						
		T44	pTis	++						
		T45	pT2−3	+						
		T46	pTa	+						
		T47	pT1	+						
		T48	pTis	++						
		T49	pTa	−						
		T50	pT2−3	+						
		T51	pT2−3	++						
		T52	pT2−3	−						
		T53	pTa	−						
		T54	pT1	−						
		T55	pTa	−		NE				
		T56	pTa	−						
		T57	pTa	−						
		T58	pT2−3	++		NE				
		T59	pT1	++						
		T60	pTis	+						
		T61	pT2−3	+						
		T62	pTis	++						
		T63	pT2−3	+						

FIG. 3. DNA methylation profiles for CpG islands and protein expression levels of DNMT1 in specimens in which 5 or all 6 CpG islands could be evaluated. DNA methylation status was examined by MSP or COBRA (fig. 2). DNMT1 protein expression levels were defined as described. Vertical columns indicate specimen number, invasion depth in TCC specimens and protein expression of DNMT1. Top row indicates CpG islands. Filled box indicates methylated. Open box indicates unmethylated. *NE*, not evaluable.

significantly higher in nonpapillary than in papillary carcinomas (chi-square test p = 0.0143). Among nonpapillary carcinomas there was no significant difference in the incidence of CIMP between flat CIS (pTis in 7 or 12 specimens or 58%) and invasive carcinomas (pT1 or greater in 20 of 26 or 77%) (chi-square test p = 0.2402).

Correlation between DNA methylation status on multiple CpG islands and DNMT1 protein expression during multistage urothelial carcinogenesis. We have previously reported

the results of immunohistochemical examination for DNMT1 in 89 of the current 105 specimens.[7] We subjected the remaining 16 specimens to the same immunohistochemical examination for DNMT1. DNMT1 immunoreactivity of a tissue sample was considered positive (+) if more than 30% of cells showed the same nuclear staining intensity as positive internal control lymphocytes, and strongly positive (++) if more than 30% of cells showed stronger intensity, as described previously.[7] Figure 3 shows the intensity of DNMT1 immunoreactivity in the 86 specimens for which DNA methylation status on 5 or all 6 CpG islands could be evaluated. In 86 specimens of normal urothelium, NBC and TCC concurrent DNA hypermethylation on 3 or more CpG islands significantly correlated with increased (+ or ++) DNMT1 protein expression (chi-square test $p = 0.0167$).

DISCUSSION

The incidence of aberrant DNA hypermethylation, such as concurrent DNA methylation on 3 or more CpG islands, was significantly higher in NBCs than in normal urothelium. TCCs are notorious for their clinical features of multicentricity and tendency toward recurrence. Synchronously or metachronously multifocal TCCs often develop in certain patients. Although multifocal development of TCCs may be partly attributable to intraluminal seeding, a possible mechanism for multiplicity is the field effect, whereby carcinogenic agents in urine cause malignant transformation of multiple urothelial cells.[12] Even noncancerous urothelium showing no remarkable histological changes can be considered precancerous, because they may be exposed to carcinogens in the urine. Our data suggest that aberrant DNA hypermethylation on multiple CpG islands may participate even in precancerous conditions during multistage urothelial carcinogenesis.

CIMP did not correlate with TCC aggressiveness (eg depth of invasion) but it significantly correlated with morphological structure (papillary vs nonpapillary). Bladder carcinomas are classified as papillary or nodular according to their macroscopic configurations. Papillary carcinomas usually remain noninvasive, although patients must undergo repeat cystoscopic resection because of recurrences.[13] In contrast, the clinical outcome of nodular invasive carcinomas is poor.[13] Flat CIS, which frequently spreads widely and is sometimes scattered over the bladder, is associated with nodular invasive carcinomas. Frequent *p53* gene mutations[14] and loss of heterozygosity on chromosome 14q[15] indicated a common background for flat CIS and invasive carcinomas and, therefore, flat CIS is considered a precursor of nodular invasive carcinomas of the bladder. In this study we successfully examined DNA methylation status even in flat CIS, which was macroscopically indistinguishable from noncancerous urothelium, using microdissection techniques. Our results suggest that CIMP is particularly associated with the development of flat CIS and nodular invasive carcinomas with a poorer prognosis.

DNMT1 targets replication foci, where DNA methylation patterns are copied from the mother strand, by binding to PCNA.[16] However, excessive amounts of DNMT1, which cannot target replication foci, may participate in de novo methylation of CpG islands that are not methylated in normal cells. In addition, targeting of substrate DNA by DNMT1 may be disrupted by mechanisms, such as dysfunction of p21WAF1,[17] which competes with DNMT1 for binding to PCNA, in cancer cells.[16] Moreover, it was recently suggested that DNMT1 is capable of de novo methylating activity as well as having a maintenance function.[18,19] Therefore, it is feasible that in cancers DNMT1 participates in regional DNA hypermethylation on CpG islands. The incidence of concurrent DNA hypermethylation on 3 or more CpG islands significantly correlated with increased DNMT1 protein expression in all examined specimens of normal urothelium, NBC and TCC, suggesting the possibility that the previously proven DNMT1 over expression actually resulted in frequent regional DNA hypermethylation during urothelial carcinogenesis.

DNMT1 mRNA is expressed mainly during the S-phase.[1] Because tumor tissue presumably contains a greater proportion of dividing cells than normal tissue does, it has been debatable whether increased DNMT1 expression is due to an increase in the proportion of dividing cells or to an acute increase in DNMT1 expression per individual cell.[20] However, we have previously reported that DNMT1 expression levels are already increased in NBCs in which the PCNA labeling index has not yet increased.[7] Increased DNMT1 expression did not result entirely from increased numbers of dividing cells in the tissues examined, but rather it clearly preceded increased cell division.[7] In our current study the incidence of concurrent DNA methylation on 3 or more CpG islands was significantly higher in NBCs than in normal urothelium, in parallel with the previously proven DNMT1 over expression. Moreover, the frequent regional DNA hypermethylation observed in our current study and the previously proven DNMT1 over expression were associated with the pathway of development of CIS and nodular invasive carcinomas. These data further support the concept that the previously proven DNMT1 over expression resulted in frequent regional DNA hypermethylation during urothelial carcinogenesis.

In our previous study in nonpapillary carcinomas DNMT1 protein expression was significantly higher in flat CIS than in invasive carcinomas.[7] On the other hand, in our current study there was no difference in the incidence of CIMP between flat CIS and invasive carcinomas. After markedly over expressed DNMT1 induces de novo DNA hypermethylation on multiple CpG islands at the stage of flat CIS, aberrant DNA methylation status may be maintained successfully even if DNMT1 expression is decreased to some extent in invasive carcinomas.

Although DNMT1 is a major DNA methyltransferase in humans, to date 2 other enzymes, namely DNMT3a and DNMT3b, have also been shown to possess DNA methyltransferase activity.[1] Genomic methylation patterns may be established through cooperation among these 3 enzymes even in cancer cells.[19] Further studies of how cooperation between DNMT1 and other components of the DNA methylation machinery affects DNA methylation status in tissue specimens may increase our understanding of the basis of regional DNA hypermethylation during urothelial carcinogenesis.

REFERENCES

1. Jones, P. A. and Baylin, S. B.: The fundamental role of epigenetic events in cancer. Nat Rev Genet, **3:** 415, 2002
2. Maruyama, R., Toyooka, S., Toyooka, K. O., Harada, K., Virmani, A. K., Zochbauer-Muller, S. et al: Aberrant promoter methylation profile of bladder cancer and its relationship to clinicopathological features. Cancer Res, **61:** 8659, 2001
3. Horikawa, Y., Sugano, K., Shigyo, M., Yamamoto, H., Nakazono, M., Fujimoto, H. et al: Hypermethylation of an E-cadherin (CDH1) promoter region in high grade transitional cell carcinoma of the bladder comprising carcinoma in situ. J Urol, **169:** 1541, 2003
4. Toyota, M., Ahuja, N., Ohe-Toyota, M., Herman, J. G., Baylin, S. B. and Issa, J. P.: CpG island methylator phenotype in colorectal cancer. Proc Natl Acad Sci USA, **96:** 8681, 1999
5. Kanai, Y., Ushijima, S., Kondo, Y., Nakanishi, Y. and Hirohashi, S.: DNA methyltransferase expression and DNA methylation of CpG islands and peri-centromeric satellite regions in human colorectal and stomach cancers. Int J Cancer, **91:** 205, 2001
6. Etoh, T., Kanai, Y., Ushijima, S., Nakagawa, T., Nakanishi, Y., Sasako, M. et al: Increased DNA methyltransferase 1

(DNMT1) protein expression correlates significantly with poorer tumor differentiation and frequent DNA hypermethylation of multiple CpG islands in gastric cancers. Am J Pathol, **164:** 689, 2004
7. Nakagawa, T., Kanai, Y., Saito, Y., Kitamura, T., Kakizoe, T. and Hirohashi, S.: Increased DNA methyltransferase 1 protein expression in human transitional cell carcinoma of the bladder. J Urol, **170:** 2463, 2003
8. Sobin, L. H. and Wittekind, C. H.: TNM Classification of Malignant Tumors, 5th ed. New York: Wiley-Liss, Inc., 1997
9. Herman, J. G., Graff, J. R., Myohanen, S., Nelkin, B. D. and Baylin, S. B.: Methylation-specific PCR: a novel PCR assay for methylation status of CpG islands. Proc Natl Acad Sci USA, **93:** 9821, 1996
10. Xiong, Z. and Laird, P. W.: COBRA: a sensitive and quantitative DNA methylation assay. Nucleic Acids Res, **25:** 2532, 1997
11. Satoh, A., Toyota, M., Itoh, F., Kikuchi, T., Obata, T., Sasaki, Y. et al: DNA methylation and histone deacetylation associated with silencing DAP kinase gene expression in colorectal and gastric cancers. Br J Cancer, **86:** 1817, 2002
12. Harris, A. L. and Neal, D. E.: Bladder cancer—field versus clonal origin. N Engl J Med, **326:** 759, 1992
13. Friedell, G. H., Parija, G. C., Nagy, G. K. and Soto, E. A.: The pathology of human bladder cancer. Cancer, **45:** 1823, 1980
14. Spruck, C. H., 3rd, Ohneseit, P. F., Gonzalez-Zulueta, M., Esrig, D., Miyao, N., Tsai, Y. C. et al: Two molecular pathways to transitional cell carcinoma of the bladder. Cancer Res, **54:** 784, 1994
15. Chang, W. Y., Cairns, P., Schoenberg, M. P., Polascik, T. J. and Sidransky, D.: Novel suppressor loci on chromosome 14q in primary bladder cancer. Cancer Res, **55:** 3246, 1995
16. Chuang, L. S., Ian, H. I., Koh, T.W., Ng, H. H., Xu, G. and Li, B. F.: Human DNA-(cytosine-5) methyltransferase-PCNA complex as a target for p21WAF1. Science, **277:** 1996, 1997
17. Baylin, S. B.: Tying it all together: epigenetics, genetics, cell cycle and cancer. Science, **277:** 1948, 1997
18. Vertino, P. M., Yen, R. W., Gao, J. and Baylin, S. B.: De novo methylation of CpG island sequences in human fibroblasts overexpressing DNA (cytosine-5-)-methyltransferase. Mol Cell Biol, **16:** 4555, 1996
19. Rhee, I., Bachman, K. E., Park, B. H., Jair, K. W., Yen, R. W., Schuebel, K. E. et al: DNMT1 and DNMT3b cooperate to silence genes in human cancer cells. Nature, **416:** 552, 2002
20. Lee, P. J., Washer, L. L., Law, D. J., Boland, C. R., Horon, I. L. and Feinberg, A. P.: Limited up-regulation of DNA methyltransferase in human colon cancer reflecting increased cell proliferation. Proc Natl Acad Sci USA, **93:** 10366, 1996

Laboratory Investigation (2005) 85, 895–907
© 2005 USCAP, Inc All rights reserved 0023-6837/05 $30.00
www.laboratoryinvestigation.org

Loss of blood group A antigen expression in bladder cancer caused by allelic loss and/or methylation of the *ABO* gene

Yoshitomo Chihara[1,2], Kokichi Sugano[1], Ayumi Kobayashi[1], Yae Kanai[3], Hidenobu Yamamoto[4], Masaaki Nakazono[4], Hiroyuki Fujimoto[5], Tadao Kakizoe[5], Kiyohide Fujimoto[2], Setsuo Hirohashi[4] and Yoshihiko Hirao[2]

[1]*Oncogene Research Unit/Cancer Prevention Unit, Tochigi Cancer Center Research Institute, Tochigi, Japan;* [2]*Department of Urology, Nara Medical University, Nara, Japan;* [3]*Pathology Division, National Cancer Center Research Institute, Tokyo, Japan;* [4]*Department of Urology, Tochigi Cancer Center Hospital, Tochigi, Japan and* [5]*Department of Urology, National Cancer Center Hospital, Tokyo, Japan*

Loss of ABO blood group antigen expression has been reported in transitional cell carcinoma (TCC) of the bladder. Synthesis of the ABO blood group antigen was genetically determined by allelic variants of the *ABO* gene assigned on 9q34.1. We analyzed loss of heterozygosity (LOH) and promoter hypermethylation of the *ABO* gene in TCC and compared them with alterations of A antigen expression in TCC, dysplasia and normal urothelium. A total of 81 samples of TCC of the bladder obtained from transurethral resection (TUR) ($n=44$) and radical cystectomy ($n=37$) were examined. Expression of the A antigen was evaluated by immunohistochemical staining (IHC) using anti-A antigen monoclonal antibody. LOH of the *ABO* gene locus was examined by blunt-end single-strand DNA conformational polymorphism (SSCP) analysis using flouresence-based auto sequencer. Promoter hypermethylation of the *ABO* gene were examined by bisulfite PCR-SSCP (BiPS) analysis and/or methylation-specific PCR (MSP). Loss of A allele and/or hypermethylation were significantly associated with abnormal expression of the A antigen in cases undergoing TUR ($P=0.02$) and radical cystectomy ($P=0.0005$). For the analysis of the concomitant dysplasia in 23 cases with TCC of the bladder, the expression of the A antigen was maintained, regardless of the A allelic loss or methylation status in the tumor. In conclusion, A allelic loss and hypermethylation in the promoter region of the *ABO* gene showed significant correlation with reduction of A antigen expression in TCC, while the expression of the A antigen is maintained in concomitant dysplasia or normal urothelium, suggesting that loss of the *ABO* gene and/or its promoter hypermethylation is a specific marker for TCC.

Laboratory Investigation (2005) **85,** 895–907. doi:10.1038/labinvest.3700268; Published online 9 May 2005

Keywords: bladder cancer; *ABO* gene; LOH; promoter hypermethylation; dysplasia

Superficial bladder cancers often show multifocal occurrences or metachronous recurrence after transurethral resection (TUR), and eventually develop into invasive bladder cancer. Allelic loss on chromosome 9 is the most frequent genetic event in transitional cell carcinomas of the bladder,[1–4] that is observed in 70% of invasive bladder cancers and even in 50% of superficial bladder cancers at Stage G1.[4] Whether or not loss on chromosome 9 arises in urothelial lesions such as dysplasia is crucial to the understanding of early genetic events in bladder carcinogenesis. Some authors have reported on the allelic loss of chromosome 9 that occurs in the small urothelial lesions and normal bladder urothelium in their attempts to trace genetic alterations using microsatellite markers.[5,6] However, it is still difficult to analyze allelic status in small epithelial regions obtained from formalin-fixed, paraffin-embedded tissues, and a few data have been reported regarding early genetic alterations in bladder dysplasia.[3,7] ABO (H) blood group antigens are constitutively expressed on epithelial cells such as those found in the gastrointestinal tract and urothelium. A reduction in blood-group A antigen (GalNAcα1-3[Fucα1-2]Galβ1-3GlcNAc-R) expression was reported in transitional cell carcinoma (TCC) of the bladder

Correspondence: Dr K Sugano, MD, PhD, Oncogene Research Unit/Cancer Prevention Unit, Tochigi Cancer Center Research Institute, 4-9-13 Yohnan, Utsunomiya-shi, Tochigi Pref. 320-0834, Japan.
E-mail: ksugano@tcc.pref.tochigi.jp
Received 16 April 2004; revised 1 January 2005; accepted 14 January 2005; published online 9 May 2005

and showed significant correlation with an invasive phenotype.[8–11] Orntoft and Wolf[12] examined the correlation between blood-group antigen expression and the activity of glycosyltransferases in TCC of the bladder and reported that the activity of A glycosyl transferase was severely reduced in tumors showing loss of A antigen expression. This phenomenon drew our attention, due to the fact that the determinant of the ABO blood-group antigen is synthesized by the action of the *ABO* gene encoding ABO glycosyltransferase assigned to chromosome 9q34.1, where loss of heterozygosity (LOH) was frequently reported in bladder cancer.[1–4] The *ABO* gene is composed of seven exons and six introns and encodes ABO glycosyltransferase, of which substrate specificity is determined by genetic polymorphisms in exons 6 and 7 (Figure 1).[13,14] Blood-group A antigen is synthesized by α-*N*-acetylgalactosaminyltransferase (A-GalNAc transferase), which catalyzes the transfer of *N*-acetylgalactosamine to the subterminal β-galactosyl residue of the blood-group H carbohydrate chain. Blood-group B-antigen is synthesized by B-galactosyl transferase, which catalyzes the transfer of galactose to the subterminal β-galactosyl residue of the blood-group H carbohydrate chain. The *ABO* gene in blood-group O donors lacks glycosyltransferase activity, for it has a deletion on a guanine residue at the nucleotide position 261 in exon 6, causing protein truncation at codon 117.[13–16] Immunohistochemistry using anti-A monoclonal antibody in bladder cancer may be useful to evaluate the allelic status of the *ABO* gene locus at 9q34.1 in those who are heterozygous for ABO genotypes. Expression of blood-group A antigen is stable enough even in formalin-fixed paraffin-embedded specimens, and this could be applicable in the analysis of small lesions that are too small to be examined by genetic analysis. Two papers were so far reported as to the correlation between reduced expression of A antigen and A allelic loss in TCCs of the bladder.[17,18] Meldgaard *et al*[17] analyzed 22 bladder tumors for LOH of the 9q allele by PCR-restriction fragment length polymorphism (RFLP) analysis of the *ABO* locus at 9q34. Seven tumors from heterozygous informative individuals were sorted by flowcytometry. LOHs were detected in the most aneuploid subpopulation of cells in two cases, but both cases were losing O-alleles. No LOHs were detected in analysis of the low aneuploid subpopulation. As all tumors showed loss of blood group ABH antigen expression, they concluded that LOH of the *ABO* locus on chromosome 9q34 is not the cause of loss of blood group ABH expression in human bladder cancer.[17] Orlow *et al*[18] analyzed 19 patients with bladder cancer serologically typed as blood group A. Expression of A antigen was maintained in 14 samples in normal urothelium, while it was reduced in nine tumors. PCR-RFLP analysis showed loss of the A allele in one tumor sample showing reduced expression of the A antigen. They indicated that the lack of the A antigen expression in certain bladder tumors is due to the allelic loss of the *ABO* gene and that in some of these tumors, the loss involved the surrounding chromosomal region at 9q34.1–4.[18] These two reports did not support the correlation between A-allelic loss and the reduced expression of the A antigen in the majority of bladder cancers. Recent advance in cancer epigenetics shed light on the reduced expression of A antigen in malignant cells. Kominato *et al*[19,20] reported that hypermethylation of the promoter region of the *ABO* gene induced *ABO* gene silencing in their study using a human stomach carcinoma cell line. Iwamoto *et al*[21] established subclones with positive or negative expression of the A antigen from parental colonic cancer cell lines and reported a distinct difference in the methylation pattern of the CpG island of the promoter region of the ABO glycosyltransferase, that is densely methylated in a subclone lacking the expression of the A antigen. Gao *et al*[22] examined 30 oral squamous carcinomas for expression of the A and B antigens and A/B glycosyltransferase, together with LOH at the *ABO* locus and hypermethylation of the *ABO* gene promoters. Loss of A or B antigen expression was found in 21 of 25 tumors (84%), while the expression of the glycosyltransferase was absent in all of tumors showing negative expression of A or B antigens. Loss of the A or B allele was found in 3/20 tumors (15%) heterozygous for the *ABO* locus and hypermethylation of the promoter region in 10 of 30 tumors (33.3%).[22] Furthermore, Habuchi *et al*[23] reported that the region 9q32–9q33, which is in the vicinity of the *ABO* gene locus at 9q34.1, is a frequent target of LOH and methylation in bladder cancer. These findings prompted us to hypothesize that deletion of blood-group A antigen expression in TCC of the bladder might be regulated by a combination of genetic and epigenetic mechanisms, that is, an LOH of the *ABO* gene locus and hypermethylation of the *ABO* gene promoter region. The purpose of this study was to elucidate the relevant mechanisms underlying the loss of blood group A antigen expression in TCC of the bladder and whether it could be used as a phenotypic marker to estimate any underlying genetic and epigenetic abnormalities in normal urothelium and concomitant bladder dysplasia in patients with bladder cancer.

Materials and methods

Samples and DNA Extraction

A total of 81 cases of TCC of the bladder were studied, of which 44 underwent TUR and 37 underwent radical cystectomy (Table 1). The histo-blood group for all cases was A (72 cases) or AB (nine cases) examined by routine hemagglutination tests at hospital. Tumors were graded and staged according to the WHO classification or the 1997 UICC TNM classification system. Based on patients'